Aus der Radiologischen Universitätsklinik Tübingen

Abteilung Diagnostische und Interventionelle Neuroradiologie

Comparative Evaluation of Prognostic Value of Arterial Spin Labelling and Dynamic Susceptibility Contrast-Enhanced MR Imaging in High-Grade Gliomas

Inaugural-Dissertation

zur Erlangung des Doktorgrades

der Medizin

der Medizinischen Fakultät

der Eberhard Karls Universität

zu Tübingen

vorgelegt von

Rau, Mandy Kim

2018

Dekan: Professor Dr. I. B. Autenrieth

1. Berichterstatter: Professor Dr. S. Bisdas

2. Berichterstatter: Professor Dr. U. Kramer

3. Berichterstatter: Professor Dr. U. Ernemann

Tag der Disputation 18.01.2018

Content

List of abbreviations

AE	Adverse event
AIF	Arterial input function
ASL	Arterial spin labelling
AUC	Area under the curve
BBB	Blood brain barrier
CBF	Cerebral blood flow
CBV	Cerebral blood volume
DSC	Dynamic susceptibility contrast-enhanced
DNA	Deoxyribonucleic acid
DWI	Diffusion weighted imaging
FLAIR	Fluid attenuated inversion recovery
KPS	Karnofsky performance score
MGMT	O-6-methylguanine deoxyribonucleic acid methyltransferase
MR	Magnetic resonance
MRI	Magnetic resonance imaging
MTT	Mean transit time
PFS	Progression free survival
QUIPS II /Q2TIPS	Quantitative imaging of perfusion using a single subtraction, version II
rCBF	Relative cerebral blood flow
rCBV	Relative cerebral blood volume
ROC	Receiver Operating Characteristic
ROI	Region-of-interest
SNR	Signal to noise ratio
TTR	Time to recurrence
WHO	World Health Organization

List of tables

List of figures

1. Introduction

The most common primary brain tumours are gliomas which originate from glial brain cells. The latest World Health Organization (WHO) classification from 2007 of gliomas includes the following histological types (1):

- Grade 1: subependymal giant cell astrocytoma and pilocytic astrocytoma,
- Grade 2: pilomyxoid, diffuse astrocytoma and pleomorphic xanthoastrocytoma
- Grade 3: anaplastic astrocytoma
- Grade 4: glioblastoma, giant cell glioblastoma and gliosarcoma.

The grade 4 neoplasms are characterized by microvascular proliferation and necrosis (1). The treatment management of the patients is mainly dependent on the histopathological grade, which determines the patient's response to therapy as well as the prognosis. In contrast to patients with WHO grade 2 tumours, who usually survive longer than 5 years (1), the prognosis in patients with high-grade gliomas (WHO grade 3 and 4) still remains poor. The standard therapeutic regimes in these patients include concomitant adjuvant radiotherapy (2) and chemotherapy. Among the available chemotherapeutic agents, temozolomide is the most widely used and its impact on the median survival in patients with glioblastoma has been reported to be 14.6 months while the median progression-free survival was only 6.9 months (3). Other prognostic criteria next to histological grade are tumour volume, localization, age at diagnosis, sex, gene expression (4, 5), Karnofsky Performance Score (KPS) (6), radiological contrast enhancement as indication of disrupted blood brain barrier (BBB) (7) and the extent of surgery and radiation dose (8). Small tumour size and more extensive tumour resection are associated with better survival. (6, 9) For this reason and because of the risk of sampling error, an open resection is generally preferred rather than stereotactic biopsy if age, tumour type and localization of the lesion allow for it. If an invasive tumour is located in a sensitive area (for example in the brain stem), an extensive and complete tumour resection in most cases cannot be guaranteed. Therefore both the time

to tumour recurrence and death is shorter than for patients with tumours located in an area like the cerebellum which allows complete resection without damaging brain function in a great extent. (6) Younger age at diagnosis of a glioblastoma has been announced as an independent factor with improved survival outcome (6, 9). Not only do glioblastomas appear more often in male patients, they also have a poorer survival rate than in female patients (10). Sun et al. showed that the cause of that observation lies in the retinoblastoma protein, which reduces cancer risk and is less active in male brain cells than in female brain cells (11). In glioblastomas MGMT (O6-alkylguanine deoxyribonucleic acid alkyltransferase) promotor gene methylation is an important prognostic factor, since is determines the response to temozolomide chemotherapy (12). If the MGMT promotor is methylated, it is inactive, thus the DNA (deoxyribonucleic acid) repair enzyme cannot be produced. If the malignant cell has contact to temozolomide, which damages the DNA, it cannot repair itself and dies. The Karnofsky performance score is a scale running from 100 (no complaints) to 0 (death) and was designed in order to quantify cancer patients' ability to manage daily life. It considers the degree of assistance a patient needs and is therefore also used as a measure of quality of life. Generally, a higher score correlates with long progression free survival (13, 14).

Patients with high grade gliomas face typical symptoms such as fatigue, uncertainty about the future, motor dysfunction, drowsiness, communication deficit and headache (15). Some symptoms are associated with the increased intracranial pressure such as nausea and vomiting, headache, fatigue, seizures and anorexia. Other symptoms derive from therapy itself such as fluid retention, weight gain, muscle weakness, osteoporosis and reduce of neurocognitive function (15-17) from corticosteroids, which are used to decrease intracranial edema. Radiotherapy causes symptoms like hair loss, fatigue, somnolence and decrease of neurocognitive function (18). Combination of radiotherapy with temozolomide leads to increased vomiting, anorexia, constipation and fatigue (19). Indeed, patients who respond to temozolomide report an improvement of quality of life (19). Of course the results of neurological damage like motor

deficits, speech or visual difficulties have an effect on disease burden, but patients suffer even more from neuropsychiatric and neurocognitive symptoms like personality changes, mood disturbances or decrease of concentration (15). Patients with high grade gliomas report at time of recurrence greater neurological deficits and suffer more often from visual problems, pain and cognitive deterioration. The latter precede radiographic evidence of progression by almost 6 weeks (20). Since patients with recurrent gliomas carry a higher symptom burden compared to patients with newly diagnosed gliomas (15), the time between first diagnosis and tumour recurrence is essential for these patients. Holding in mind the above mentioned side effects of therapy and their influence on quality of life, possible therapy has to be carefully balanced with patients' prognosis of progression free survival. The investigation of the prognostic value of a non-invasive imaging technique is therefore of great interest for therapy decisions.

Conventional magnetic resonance imaging (MRI) has been the reference imaging modality to distinguish between the different types of gliomas. Low-grade gliomas are typically well demarcated and show high signal intensity on T2-weighted imaging, low signal intensity on T1-weighted imaging and usually no contrast-enhancement. Anaplastic astrocytomas share features of both diffuse astrocytoma and glioblastoma, possibly gadolinium enhancing, and they usually show some mass effect. Glioblastomas are typically irregularly shaped enhancing masses with diffuse borders and infiltrating outliers (Figure 1). They usually include necrotic parts and cysts (21).

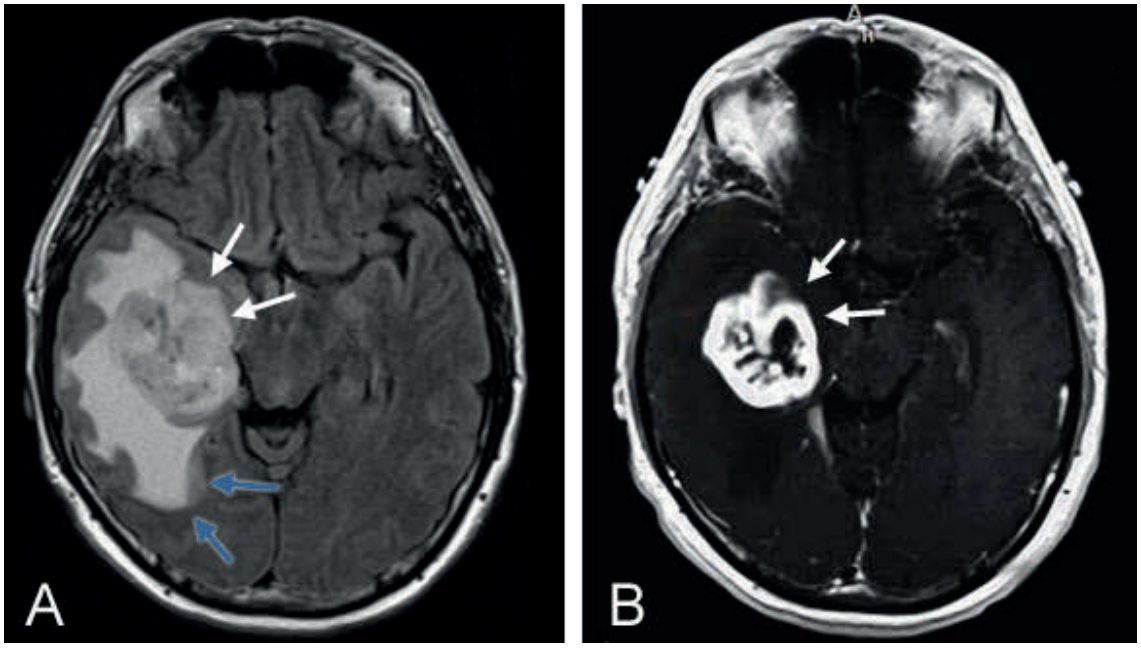

Figure 1: MRI of a patient with right temporal glioblastoma.
(A) shows the FLAIR sequence of a right temporal glioblastoma (indicated with white arrows) with peritumoural oedema (blue arrows), which indicates typical infiltration. (B) shows the contrast-enhanced T1-weighted image. It demonstrates strong enhancement of the tumour mass with central necrotic parts (white arrows) which hints of blood brain barrier disruption and is also a typical feature of glioblastomas.

Nevertheless, conventional magnetic resonance (MR) neuroimaging may still fail to distinguish WHO grade 1-2 from 3-4 tumours, a shortcoming that carries obvious therapeutic implications. Cofounding perifocal oedema poses also a diagnostic challenge since it is impossible to differentiate it from infiltrating or relapsing tumour tissue, either at the baseline diagnosis or during surveillance. Such drawbacks of conventional MRI have been partly overcome by advanced MRI techniques including mainly tissue perfusion imaging. Perfusion MRI is not grounded on the strict definition of perfusion as measure of the delivery of nutritional agents via blood to brain tissue parenchyma per unit per minute (2), but it encompasses several perfusion surrogates such as cerebral blood volume (CBV), cerebral blood flow (CBF), mean transit time (MTT) and contrast agent leakage. These perfusion parameters may be estimated by means of T1-, T2*-weighted dynamic contrast-enhanced acquisitions as well as by arterial spin labelling (ASL).

1.1 T2*-weighted dynamic susceptibility contrast-enhanced MRI

T2*-weighted DSC MRI has been utilized in neuro-oncology to assess the degree of angiogenesis and BBB-disruption in gliomas, which is an important feature for tumour grading (22, 23), as well as a prognostic factor to therapy response and survival (24, 25). The technique is based on the rapid injection of gadolinium chelates with high magnetic susceptibility through a peripheral vein. Given a faultless BBB, the contrast agent stays due to its size and low lipophilicity in the intravascular space. Thus, DSC imaging can be used to determine the integrity of the blood brain barrier and the degree of neovascularity, which often refers to high-grade gliomas. DSC MRI provides different perfusion-related parameters such as relative cerebral blood volume (rCBV), relative cerebral blood flow (rCBF), leakage of the contrast agent in the extravascular space, MTT of the contrast agent in the tissue of interest and k1. Leakage refers to the quantity of the extravasated contrast agent in case of disrupted BBB and k1 is the gadolinium transfer constant into the extravascular space being similar to the permeability of the vessel wall.

rCBV has been the most broadly examined perfusion parameter. The existing evidence suggests that it is superior to other perfusion parameters in predicting tumour grade (22) and it shows the best correlation to histopathologic grading (23). On the other hand, rCBV has also several limitations such as providing relative instead of absolute quantification and being prone to susceptibility artefacts. In case of severe disruption of the BBB, rCBV may be underestimated (26) and it should be *a posteriori* corrected for the contrast extravasation (27).

For the assessment of rCBF by DSC imaging, an arterial input function (AIF) is necessary and it usually refers to the vessels in the circle of Willis. To address the lack of standardisation and suboptimal technique performance due to inconsistent manually selected AIF (28), the latter can be automatically set by implemented robust software algorithms. Even if advanced post-processing (including local arterial input functions) is applied, there are some disturbing factors left, which prohibit an accurate registration of the AIF time integral and

thus, accurate quantification (29). These factors include partial volume effects, arterial signal saturation at peak concentration, large vessel signal displacement during bolus passage and different contrast agent responses in arterial blood and tissue (30).

Compared to other perfusion techniques like ASL, the inherent advantage of DSC technique resides in the increased signal from arterioles and capillaries as well as from larger vessels leading to a clinically sufficient signal to noise ratio (SNR) (31-33).

1.2 Arterial spin labelling

ASL is in contrast to DSC MRI a completely non-invasive imaging technique, which requires no exogenously administered intravascular contrast agent. Instead of that, the spins in the patient's own blood are used as an intrinsic tracer, which is magnetically labelled by means of a specific MR pre-pulse, before it enters the examined tissue volume (34). This technique offers absolute quantification (compared to the DSC MRI based relative one) of brain perfusion (in terms of blood flow) and is especially valuable for patients who need multiple scanning, e.g. for tumour therapeutic monitoring. Moreover, patients with high-risk of nephrogenic systemic fibrosis (NSF) (35), children and patients whose veins are unsuitable for contrast injections with high flow rate can benefit from the non-gadolinium-based ASL-technique. In addition, leaky immature tumour vessels, who may challenge the post-processing algorithms of DSC MRI method leading to approximations of the tracer kinetic behaviour, do not pose a relevant problem for the ASL technique, which more importantly does not rely on the AIF estimation (28). One disadvantage of ASL compared to DSC MRI is the worse signal-to-noise ratio (36). Thus, ASL acquisitions have to be lengthy in order to compensate for it. Moreover, underestimation of ASL-based rCBF may occur in regions with delayed labelled blood arrival (37), when labelled blood might not have completely reached the parenchyma up to the time of image acquisition. This sensitivity of ASL to the post labelling delay is relevant

for the perfusion estimation in elderly patients with lower/prolonged blood ejection fraction and cerebrovascular disease (28). Adversely, slow blood transit time may artificially increase the signal in the proximal arteries, which may be erroneously interpreted as neoplastic vessels in tumour patients (28) and may lead to biased perfusion quantification. This drawback has been largely overcome by crusher gradients used to suppress the signal from the slowly moving spins in the large arteries.

The ASL measurement is typically conducted at a particular inversion time, which is approximately 1200 ms at 1.5T and 1600 ms at 3T based of the T1 time decay of magnetically labelled blood (38). This selected inversion time is related to normal rather than tumourous brain tissue. At low inversion times the labelled spins are mainly located in arterial vessels. In order to achieve accurate measurements, an adequate post labelling delay time about two seconds is fundamental to allow the spins to completely enter the grey matter (39). Even longer inversion times are needed for white matter. Because of the longitudinal relaxation, the magnetization of the labelled bolus decreases at very late inversion times. Thus, higher inversion times might be of benefit, but this would also lead to a decreased SNR caused by the rapid decay of the ASL-measured perfusion signal over time. In light of these limitations, other authors have suggested that the ASL-derived intratumoural signal intensity depicts tumour circulation but not tumour perfusion and should be more precisely called “normalized vascular intratumoural signal intensity” (40).

1.3 Background and purpose

On a comparative basis, previous studies have shown that DSC MRI and ASL yield comparable perfusion values in healthy brain tissue (31, 41) as well as in brain tumours (27, 28, 42, 43). Up to date, the ASL-derived CBF estimates have initially demonstrated ability to distinguish between high- and low-grade gliomas (28, 44), but they have not been widely used for this purpose as DSC MRI derived rCBV. Adding to this, the prognostic value of the ASL-derived CBF

compared to the DSC-derived rCBF and rCBV has been less intensively investigated, yet. But since ASL holds distinct advantages over DSC MRI, the purpose of this study was to examine whether ASL-derived CBF is comparable or even superior to DSC-derived perfusion-related parameters, including rCBF, rCBV and gadolinium leakage to assess the time to recurrence in patients with high-grade gliomas. Secondarily, the intention was to compare ASL- and DSC-derived CBF values in the same population and examine whether these values may be used in an interchangeable way.

2. Materials and Methods

2.1 Patients

From February 2010 to March 2013 69 patients with histologically verified high-grade gliomas could be included in this study. These patients underwent their MRI's out of clinical routine and were retrospectively collected. Among were 39 men and 30 women. Their median age was 53 years ranging from 23 to 79 years. The median KPS was 90, ranging from 40 to 100. Among the gliomas were 59 WHO grade IV and 10 WHO grade III gliomas. The patient cohort was confined to high-grade gliomas to exclude any possible impact of the current histopathological grading system. The same therapy scheme was used for all patients: Tumour resection where possible following adjuvant chemoradiation according to Stupp protocol (3). If tumour resection is a reasonable part of therapy gets individually discussed and determined in weekly tumour boards with specialists from neurosurgery, neuroradiology, neurology and radiooncology. Material for histological verification was gained through tumour resection in 56 patients or stereotactic biopsy targeted by T1-weighted contrast enhancement or positron emission tomography (PET) data in 13 patients. The inclusion and exclusion criteria are summarised below (30):

Inclusion criteria

1) Histologically confirmed WHO Grade 3-4
2) DSC and ASL MR imaging previous to surgery and onset of therapy
3) Adequate follow-up of patients for at least 6 months after completion of adjuvant chemoradiation according to Stupp protocol (3)
4) Histological verification of any tumour recurrence

Exclusion criteria

1) Any contraindication to gadolinium or MR imaging administration
2) Imaging artefacts affecting any post-processing

3) Dropout of therapy
4) Dropout of follow-up

Twenty-two subjects showed significant mass effect in terms of midline shifting or considerable displacement of the adjacent healthy brain structures. They received 12–18 mg dexamethasone intravenously per day for up to two days prior to surgery. Among ten patients underwent MR imaging one day after initiation of the glucocorticoid therapy. This study was approved by our local ethics committee before any action on patients was taken. The ethics committee's vote is available under the reference number 27/2010B01. In addition all patients gave informed consent. (30)

2.2 Image data acquisition

Conventional MRI examinations were performed on 1.5T (Magnetom Aera; Siemens Healthcare AG, Erlangen, Germany) and 3T MRI scanners (Trio Tim; Siemens Healthcare AG, Erlangen, Germany), using a 12- or 32-channel head coils, respectively.

For the evaluation of brain tumours the standard clinical MRI protocol was used consisting of T2-weighted turbo-inversion recovery-magnitude, fast Spin Echo (FSE) T2-weighted, diffusion weighted imaging and 3D T1-weighted gradient-echo sequences before and after i.v. contrast medium application (0.1 ml/kg body weight of a gadolinium-based contrast agent called Gadovist® from Bayer Schering AG, Berlin, Germany).

2D-ASL was performed through a pulsed ultrafast echo planar imaging sequence with a single subtraction. The applied technique is called quantitative imaging of perfusion using a single subtraction, version II, (QUIPS II a. k. a. Q2TIPS) and both a thin-slice TI1 periodic saturation and a proximal inversion with control for (TR) off-resonance effects (PICORE) tagging scheme was used. QUIPS II is a modification of pulsed ASL, which decreases the sensitivity to blood transit-times by applying saturation pulse to the tagging region after the

inversion pulse and before image acquisition. In this way the trailing edge of the tagged bolus gets cut off and a sharply defined blood bolus is produced (45). For a more detailed description of this technique the reader is referred to previous work from Wong et al. (46). Following are the ASL imaging parameters for 3T: voxel size = 3.75 x 3.75 x 5 mm, slice thickness = 3 mm, intersection gap = 1 mm, T1 = 700 msec, saturation stop = 1600 msec, T2 = 1800 ms, measurement repetitions = 60. The remaining ASL imaging parameters are summarized in Table 1. In order to suppress the intravascular signal and avoid artificially high blood flow measurements when trying to quantify brain perfusion, crusher gradients were used. For gaining maximal SNR, water protons were inverted by a short radio-frequency pulse. Since patient's movement can lead to large subtraction errors (47), the patient's head was fixed with vacuum cushions in the head coil and all ASL-images were motion corrected on-site. The administration of contrast agent was unexceptionally performed after the acquisition of ASL. In eight cases, it was not possible to acquire ASL data due to patient movement or other technical failures.

Table 1: Overview of imaging parameters
Following parameters of arterial spin labelling (ASL) and dynamic susceptibility contrast-enhanced (DSC) imaging are summarized: time of repetition, echo time, field of view, flip angle, number of slices, and slice thickness. Units are in square brackets.

	Time of repetition [ms]	Echo time [ms]	Field of view [mm]	Flip angle [°]	Number of slices	Slice thickness [mm]
ASL	3000	19	240 x 240	90	9	3
DSC	1610	30	220 x 220	60	20	3

For DSC imaging a fast gradient-echo EPI sequence was used during the first pass of a bolus of gadobutrol (Gadovist®, Bayer Schering AG, Germany) with a standard dose of 0.1 ml/kg body weight at an injection rate of 4 ml/s. In order to avoid underestimation of CBF in the tumour because of leakage effects, a preloading dose of contrast agent (0.5 mmol/kg body weight) was injected with a rate of 4 ml/s before DSC imaging (48). The imaging parameters at 3T were:

matrix 128 x 128 voxel, acceleration factor 2, temporal resolution 1.5 s. For more parameters please see Table 1.

2.3 Imaging data post-processing and analysis

The DSC MRI data were transferred off-line to a dedicated post-processing workstation running the Visia™ Software (MeVis Medical Solutions AG, Bremen, Germany). The leakage correction algorithm described by Boxerman et al. (49) was used to calculate rCBV values. Therefore the original signal-intensity-curve is first converted to a relaxivity-time curve. From this the uncorrected rCBV is then calculated through integration. The leakage-corrected rCBV is then derived by applying a whole-brain estimated leakage correction term (32). Based on the corrected rCBV, rCBF maps were generated by the equation rCBF = rCBV/MTT (central volume theorem of the indicator dilution theory (50)) after calculation of the MTT assuming a bolus injection of the contrast agent (51). The resulting rCBF maps were then superimposed on anatomical T2- and T1-weighted images. Each automatically obtained AIF was manually controlled in order to assure noise-free curves with satisfactory fitting suitable to enter the post-processing and parameters calculation.

Region-of-interest (ROI) analysis was performed by placing a freehand-drawn ROI over the enhancing, macroscopically non-necrotic tumour areas (Figure 2) avoiding leptomeningeal vessels wherever possible (30). Another standardized ROI of 0.2 mm² was placed in the contralateral healthy white matter. In four cases with WHO grade 3 gliomas which showed no gadolinium enhancement, the freehand ROI placement was based on the Fluid attenuated inversion recovery (FLAIR) imaging abnormality and inevitably included also parts of the peritumoural oedema, since peritumoural infiltration may have altered rCBV values (52).

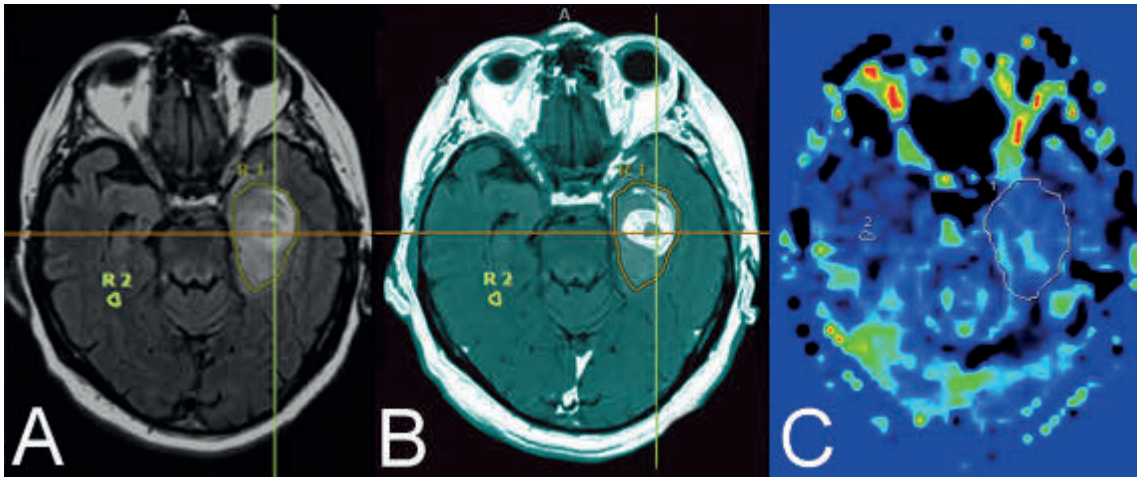

Figure 2: Example of a ROI analysis
Perfusion maps of a left temporal glioblastoma. (A) shows the FLAIR sequence with a free hand ROI drawn for better presentation around the tumour and the peritumoural oedema. Another ROI is placed in the contralateral healthy white matter. (B) shows the contrast-enhanced T1-weighted image with intratumoural enhancement. (C) shows the ASL map of CBF. The free hand ROI placement is based on the FLAIR image.

The ASL-rCBF maps were online calculated based on the General Kinetic Model according to Buxton et al. (53) after motion correction and background noise suppression. ASL-derived CBF maps were also registered on post-contrast T1-weighted images and ROI analysis was performed following the same pattern applied in DSC MR analysis (30). A proprietary workstation (Leonardo Syngo, Siemens Healthcare AG, Erlangen, Germany) was used to measure the signal intensities of the lesions on the ASL-CBF map. The intensities within the lesions were normalized based on the intensity within the contralateral healthy white matter. The perfusion parameter normalisation by calculating the ratios to the mean value of the contralateral white matter was preferred since it has been shown perform satisfactorily in tumour grading (28, 54, 55). The normalized parameters are defined as DSC-rCBV, DSC-rCBF (DSC MRI) and ASL-rCBF. Both maximum values, which are shown to provide the best intraobserver and interobserver reproducibility (28), and mean tumour values were entered into the statistical analysis. Finally, the spatial distribution of the “hot-spots”, namely the sites with the highest perfusion values within a

tumour, was visually compared between DSC-rCBF, DSC-rCBV and ASL-rCBF maps in order to assess the spatial concordance between the two techniques.

2.4 Statistical analysis

Analysis was performed using IBM® SPSS® Statistics, Version 21, Armonk, United States and MedCalc, Version 12.5.0, Ostend, Belgium for Windows. Results were declared statistically significant at the 2-sided 5 % comparison-wise significance level ($p < 0.05$).

At all variables Shapiro–Wilk test for normality was applied.

In order to compare DSC-rCBF and ASL-rCBF values Wilcoxon test and Bland Altman plot analysis were used. Wilcoxon test is a nonparametric test, which compares paired samples within a population to examine whether there is a difference of the population's mean ranks. In this case DSC-rCBF and ASL-rCBF values of every patient were compared concerning the absolute difference. Then the results were ordered by absolute difference and got a new increasing rank independent whether negative or positive. Pairs which are tied in absolute value got the average of their 2 ranks as new rank. The ranks of positive and negative differences were added together, respectively. The smaller sum is the value of W, which got proved of significance. Bland Altman plot is a graphical analysis to compare two measurements techniques. Here the differences between ASL-rCBF and DSC-rCBF values were plotted against the averages of both values.

To find any correlation for the continuous and interval scaled variables Spearman's rank correlation coefficient q was determined (30).

Receiver Operating Characteristic (ROC) curve analysis was applied to compare the prognostic value of the different perfusion parameters and to define the optimal cut-off perfusion values for prediction of time to recurrence (TTR) (30, 56). In ROC analysis the true positive rate (Sensitivity) was plotted in

function of the false positive rate (100-Specificity) for different cut-off points of a perfusion parameter. Each point on the ROC curve represents a sensitivity/specificity pair corresponding to a certain decision value. The area under the ROC curve indicates how well the perfusion parameter is able to distinguish between patients with and without an adverse event within 6 months. To perform ROC curve analysis with two combined perfusion parameters (i.e. rCBV-rCBF), binary logistic regression was conducted and the predicted probabilities from these parameters were recorded. Subsequently, they were entered as a new variable in the ROC curve analysis. Two groups were constituted, one group with high and one with low perfusion values. The value with the highest Youden index, the point in the ROC curve analysis that optimizes the parameter's differentiating ability, when equal weight is given to sensitivity and specificity was used as cut-off value.

The number of days between the first adjuvant treatment dose and the diagnosis of histologically confirmed tumour recurrence in follow-up surveillance was defined as TTR. Kaplan-Meier method with log-rank (Mantel-Cox) test was applied to calculate survival curves of the two constituted groups.

Since only a small group of patients received dexamethasone and since there was a close time between the pre-treatment scan and the therapy initiation (one day) a confounding effect of steroid doses on the perfusion values is implausible (30, 57).

3. Results

In the following the results of the study are presented. They have been partly already published in the study „Prognostic value of blood flow estimated by arterial spin labeling and dynamic susceptibility contrast-enhanced MR imaging in high-grade gliomas“ by Rau et al. (30)

Descriptive statistics contain demographic and clinical characteristics of both patients with and without an adverse event within six months; a summary of determined perfusion parameter; a summary statistic of WHO grade 3 vs. grade 4 tumours regarding PFS, KPS and perfusion parameters; mean preoperative tumour volume; the amount of patients with and without disruption of BBB and the percentage of patients with an adverse event both within six months and within the entire observation period of 37 months.

The heading “correlations” holds Spearman’s rank correlation of the different perfusion parameters.

Results regarding to comparison of DSC imaging and ASL contain Wilcoxon test and Bland-Altman method.

The spatially distribution patterns of maximum DSC-rCBV, DSC-rCBF and ASL-rCBF are presented with several imaging examples.

Results of ROC analysis containing median TTR and results of Kaplan-Meier analysis are summarized unter the headline “Survival analysis”.

3.1 Descriptive statistics

Table 2 shows demographic and clinical characteristics of both patients with an adverse event within six months and patients without an adverse event within six months. Adverse event holds either recurrence or death. There was no patient with a WHO grade 3 glioma who had an adverse event within 6 months. Eleven patients with a frontal tumour had an adverse event, 22 of them not.

Twenty-three patients with a temporal tumour had no adverse event, whereas three of them had one.

Table 2: Descriptive statistics of patients with and without adverse event (AE)
Included are median age and range in years, gender, WHO grade, Karnofsky performance score (KPS), tumour location, preoperative tumour volume (TV) in cm^3, median and range of progression free survival (PFS) in days of patients with an AE, namely recurrence or death, within six months and patients without an adverse event within six months (no AE). Median Age was similar in both groups. 45 % of female Patients had an AE and ~40 % of male had one. Interestingly no one with a grade 3 astrocytoma had an AE within 6 months. Tumours located temporal had mostly (~13 %) no AE, whereas frontal tumours led to an AE in 50 %.

	Age [years]		Gender		WHO grade		KPS [%]	
	Median	Range	Male	Female	3	4	≤ 80	> 80
No AE	53	56	29	20	10	39	12	37
AE	55	36	10	10	0	20	7	13

	Tumour location				TV [cm^3]	PFS [days]	
	Frontal	Parietal	Occipital	Temporal	Mean	Median	Range
No AE	21	5	1	22	25.38	380	846
AE	13	2	1	4	18.50	80	441

Table 3 contains the summery of both median and range of DSC-rCBV, DSC-rCBF, ASL-rCBF and leakage.

Table 3: Summery of determined perfusion parameters
Summarized are the perfusion parameters relative rCBV, rCBF and leakage of DSC imaging and rCBF of ASL.

Perfusion Parameter	Median	Range
DSC-rCBV	8.0	2.1 – 24.6
DSC-rCBF	6.9	1.5 – 18.4
ASL-rCBF	5.3	1.2 – 20.1
leakage	14.9	1.5 – 193.6

Table 4 shows a detailed summary of perfusion parameters and clinical characteristics of patients with gliomas WHO grade 3 vs. 4 gliomas.

Table 4: Summary statistics between 2 patient subgroups (grade 3 vs. 4) regarding to progression free survival (PFS), Karnofsky performance score (KPS), rCBV and rCBF measured with DSC-imaging (DSC-rCBV, DSC-rCBF), leakage and rCBF measured with ASL (ASL-rCBF). Grading is based on the World Health Organization (WHO) classification.

	PFS [days]		KPS [%]		DSC-rCBV	
	Median	Range	≤ 80	> 80	Median	Range
WHO Grade 3	670	846	0	10	7.18	8.92
WHO Grade 4	255	912	19	40	8.11	39.84
	DSC-rCBF		leakage		ASL-rCBF	
	Median	Range	Median	Range	Median	Range
WHO Grade 3	6.31	11.11	9.80	22.60	3.31	18.77
WHO Grade 4	6.99	16.97	14.88	192.05	5.84	13.29

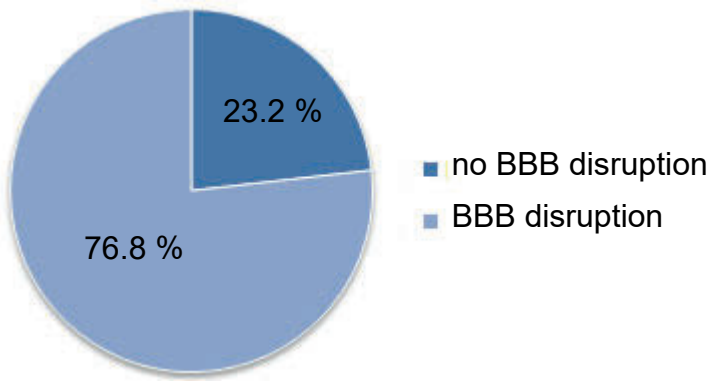

Figure 3: Pie diagram of blood brain barrier (BBB) disruption
You can see percentages of patients with and without BBB disruption before surgery. The majority had BBB disruption, being a sign of malignancy.

The mean preoperative tumour volume was 31.04 ± 24.8 cm^3 (range 5.4 – 111.3 cm^3). Before surgery 53 cases (76.8 %) showed BBB-disruption, 16 cases (23.2 %) had a non-disrupted BBB (Figure 3). Follow-up MR

examinations 24 – 48 h after surgery showed in 55 cases no residual BBB-disrupted tumour tissue. In 14 cases (20 %), residual disease (mean tumour volume 0.12 ± 0.04 cm^3, range 0.08 – 2 cm^3) was found. Twenty patients (29 %) suffered tumour recurrence within six months. Forty-four subjects (64 %) experienced recurrence during the entire observation period of 37 months (Figure 4).

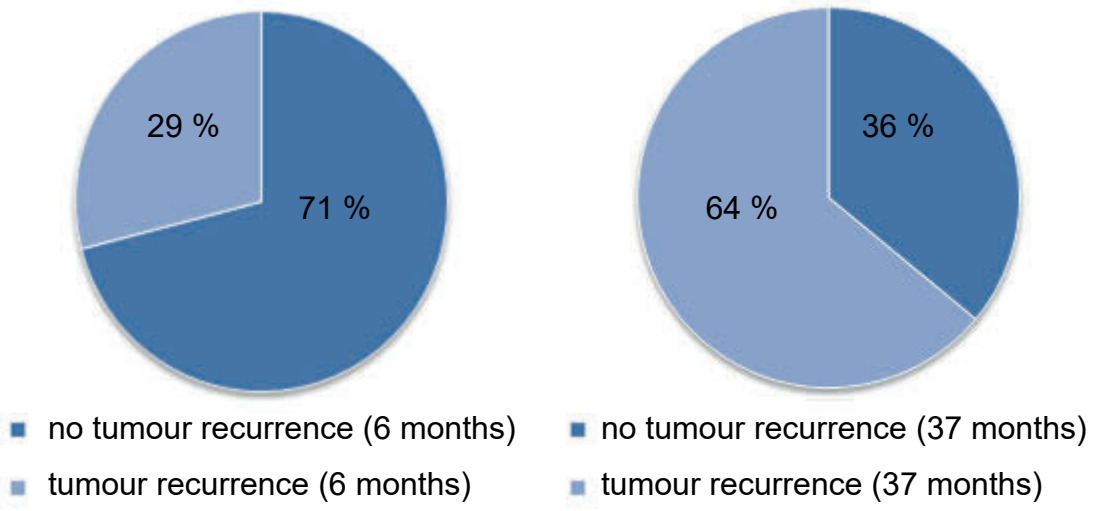

Figure 4: Pie diagrams of tumour recurrence after 6 and 37months.
These diagrams are indicating the percentages of patients with and without tumour recurrence after 6 months (left diagram) and over the whole observation period of 37 months (right diagram).

3.2 Correlations

There was no significant correlation between ASL-rCBF and DSC-rCBF ($p = 0.12$) as well as DSC-rCBV ($p = 0.7$). Spearman's rank correlation showed significant correlations between all DSC perfusion parameters as follows: rCBV-rCBF: $r = 0.61$, $p < 0.0001$*; rCBV-leakage: $r = 0.33$, $p = 0.01$*; rCBF-leakage: $r = 0.33$, $p = 0.01$*. None of the DSC perfusion parameters was significantly correlated with ASL-rCBF ($p \geq 0.80$).

3.3 Comparison of DSC imaging and ASL

Wilcoxon test indicated no significant difference between ASL-rCBF and DSC-rCBF ($p = 0.07$). Linear regression of the difference between rCBF and ASL-rCBF as dependent variable and the average between both parameters as independent variable showed proportional bias indicating that the difference between both measures is a function of the average of the measures. Plotting the differences between DSC-rCBF and ASL-rCBF against the means of DSC-rCBF and ASL-rCBF for each patient (both variables showed normal distribution) using the Bland-Altman method (Figure 5) demonstrated also that the vertical spread of the scatter points was narrower at low values of the average of DSC-rCBF and ASL-rCBF than at high values of the average of both measures. The average difference between DSC-rCBF and ASL-rCBF was 1.47. The 95 % limits of agreement (± 1.96 standard deviation) were -10.64 and 13.58.

3.4 Spatial distribution of maximum perfusion values

Qualitative comparison of perfusion maps showed different spatial distribution patterns of tumour hot spots, meaning areas of the perfusion map with maximum DSC-rCBV, DSC-rCBF and ASL-rCBF, respectively. The distribution of DSC-rCBV and DSC-rCBF was for every tumour exactly the same (Figure 6). Consequently, in the following only hot spots DSC-rCBF and ASL-rCBF was compared, the comparison with DSC-rCBV was waived. In 21 tumours the areas of maximal perfusion of DSC-rCBF and ASL-rCBF was similar and partially overlapped (Figure 7), through it was not exactly identical. In 29 tumours, the hot-spot in DSC-rCBF maps was spatially different to the hot spot of the ASL-rCBF maps (Figure 8). Only in nine tumours, the DSC-rCBF and ASL-rCBF maps showed spatial concordance (Figure 9).

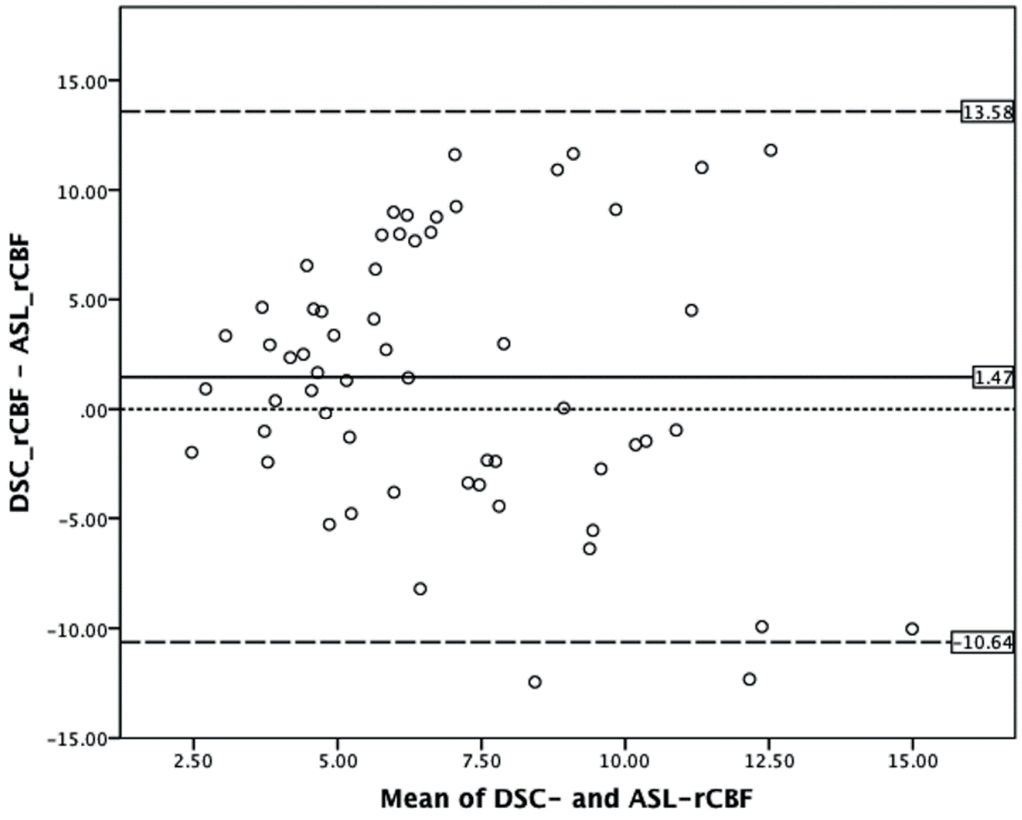

Figure 5: Bland-Altman plot of the DSC-rCBF and ASL-rCBF
Every plot shows for the corresponding patient the difference DSC-rCBF - ASL-rCBF at the mean value of these both perfusion values. The mean difference of DSC-rCBF and ASL-rCBF (depicted by the horizontal line in the diagram) is 1.47. The plot shows that the vertical spread of the scatter points is wider at high values of the average of both measures indicating a proportional bias. This means that at least one method is especially variable at high values of DSC- and ASL-rCBF. Two outliers are depicted out of the 95 % limits of agreement (±1.96 standard deviation), which are 13.58 and -10.64 (30).

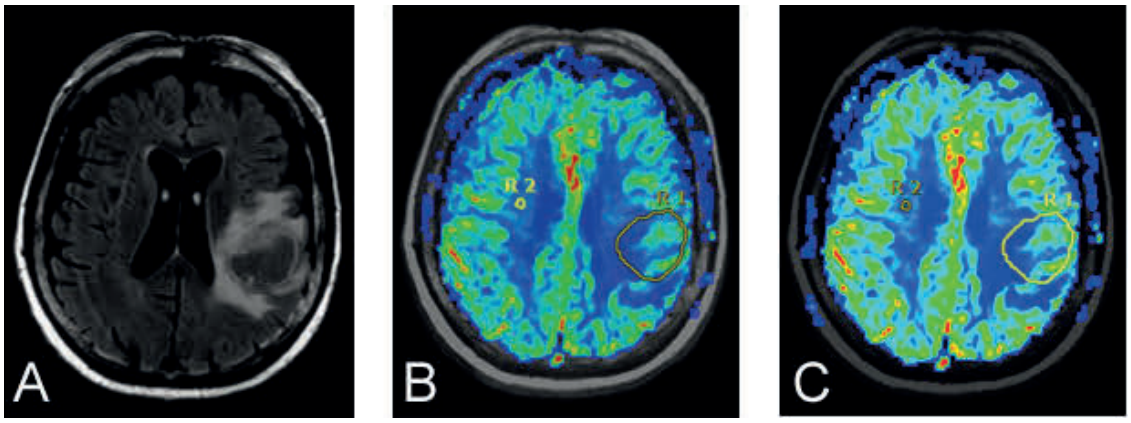

Figure 6: Example of identical spatial distribution of DSC-rCBV and -rCBF
(A) shows the FLAIR sequence of a patient with left frontoparietal glioblastoma. (B) shows the corresponding DSC-rCBF map, (C) shows the DSC-rCBV map. There is an identical spatial distribution of maximum DSC-rCBF (B) and –rCBV (C) in the tumour area (as indicated by the hand-drawn circle). This was true in all cases; therefore the comparison of DSC-rCBV with ASL-rCBF was waived.

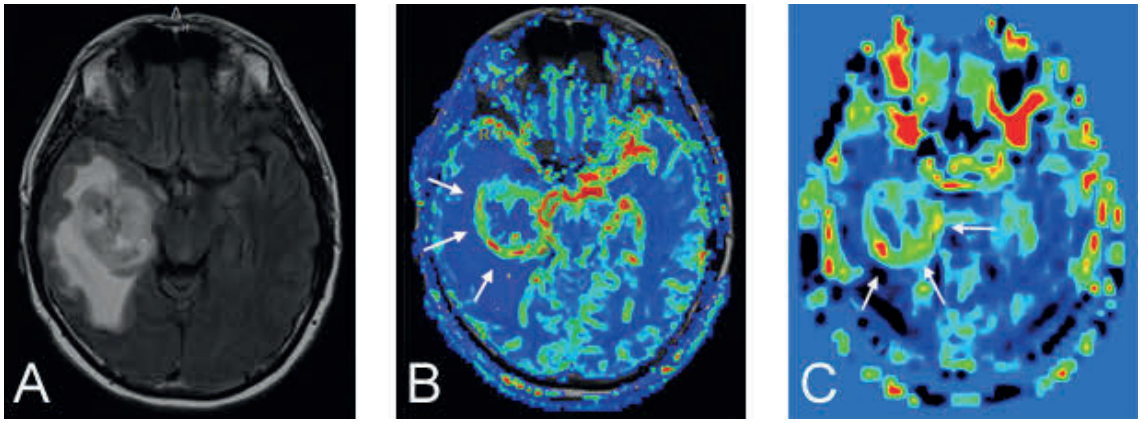

Figure 7: Example of similar spatial distribution of DSC-rCBF and ASL-rCBF
(A) shows the FLAIR sequence of a patient with right temporal glioblastoma, (B) shows the corresponding DSC-rCBF map. (C) shows the corresponding ASL-rCBF map. The DSC-rCBF map (B) and ASL-rCBF map (C) show similar spatial distribution of the maximum DSC-rCBF and ASL-rCBF values in the tumour area (as indicated by the arrows).

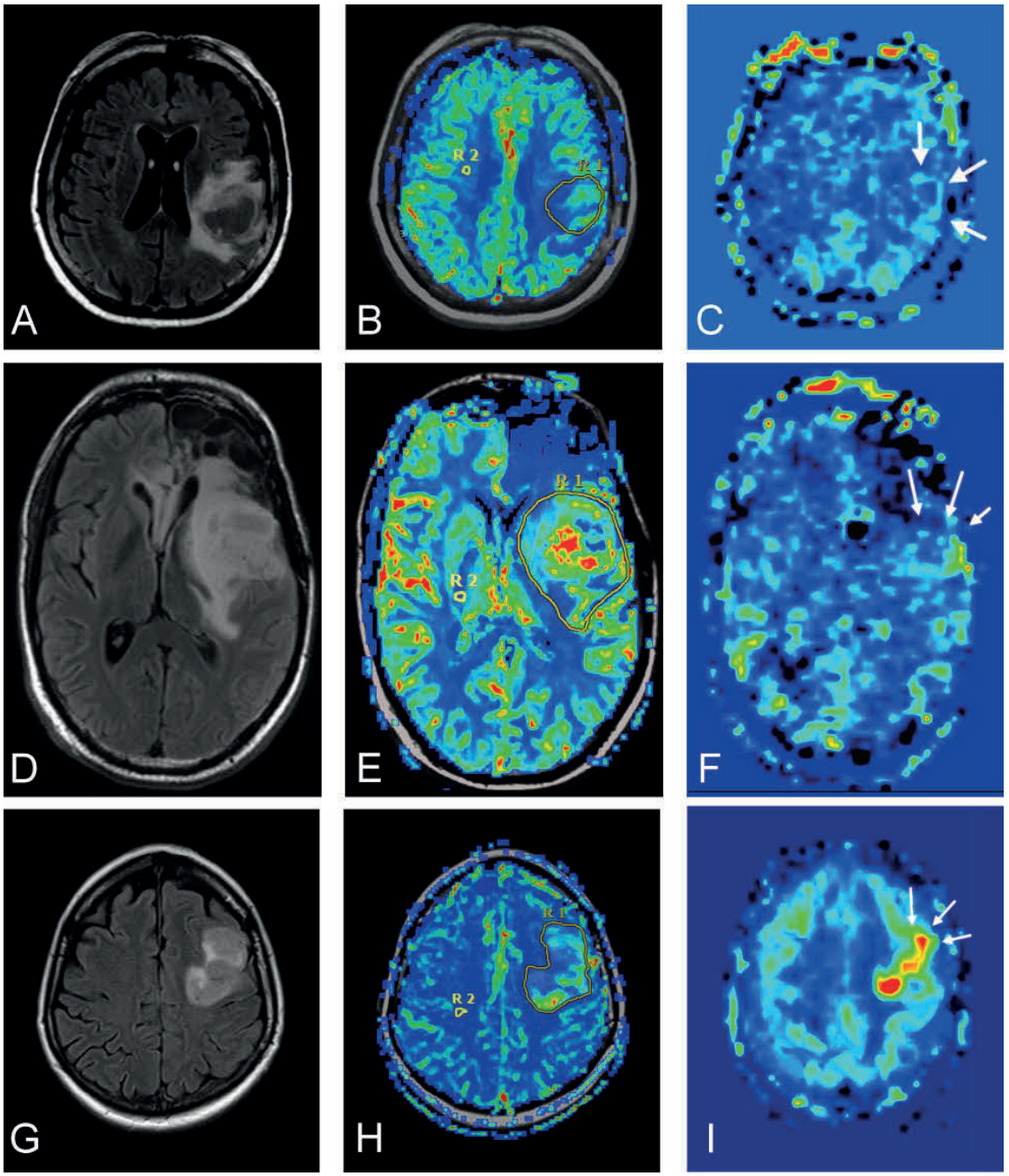

Figure 8: Example of non-similar distribution of DSC-rCBF and ASL-rCBF
Three patients (A-C), (D-F) and (G-I) with FLAIR (A, D, G), DSC-rCBF (B, E, H) and ASL-rCBF (C, F, I) maps. (A) shows the FLAIR sequence of the same patient of Figure 6 with a left frontal glioblastoma. The areas of maximum DSC-rCBF (B) values are not visually prominent in the ASL-rCBF (C) map, which shows a different, more border stressed distribution (arrows). (D) shows the FLAIR sequence of a patient with left frontal glioblastoma. In the DSC-CBF map (E) maximum values are located in the tumour centre (ROI), whereas in the ASL-rCBF map (F) the distribution of maximum values are located in the periphery of the tumour (arrows). (G) shows again the FLAIR sequence of a patient with a left frontal glioblastoma. The maximum values in the DSC-rCBF map (H) are located in the periphery of the tumour region (ROI), whereas the distribution of maximum ASL-rCBF (I) has its maximum in the tumour centre (arrows)

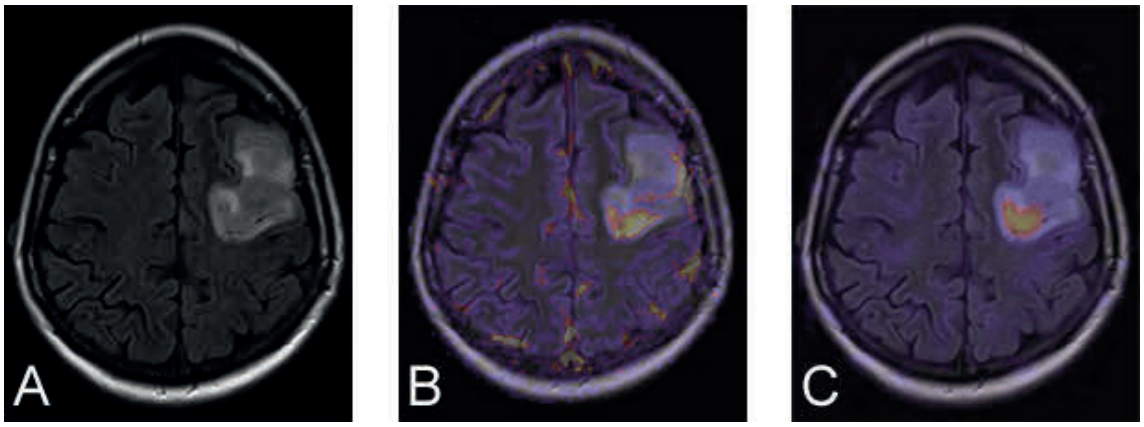

Figure 9: Example of similar distribution of DSC-rCBF and ASL-rCBF
(A) shows the FLAIR image of a patient with left frontal glioblastoma with typical irregular confirmation and attendant oedema. (B) shows the corresponding DSC-rCBF map. (C) shows the ASL-rCBF perfusion map with the same spatial distribution compared to DSC-rCBF map (B).

3.4 Survival analysis

In ROC Analysis DSC and ASL-based perfusion parameters demonstrated moderate to satisfactory prognostic values for TTR (Table 5), whereas the predictive value of DSC-rCBV with an AUC of 0.71 ($p = 0.006$) was shown to be significantly superior to ASL- and DSC-rCBF with an AUC of 0.89 ($p > 0.05$) and 0.89 ($p > 0.05$), respectively (Table 5). The combination of more than one DSC perfusion parameters increased the prognostic value of the method, while the addition of ASL-rCBF to DSC-rCBV, DSC-rCBF and leakage provided the highest AUC value of 0.74. The combination of all DSC perfusion parameters (DSC-rCBV, DSC-rCBF and leakage) achieved an AUC of 0.72 (Table 6). Notably, the combination of DSC-rCBV and ASL-rCBF presented an AUC of 0.71, which is exactly the same as the perfusion parameter which scored best in single ROC analysis, namely DSC-rCBV.

The cut-off perfusion values with the highest Youden-Index in ROC-analysis were for DSC-rCBV 6.8 (sensitivity 73 %, specificity 64 %), for DSC-rCBF 5.7 (sensitivity 75 %, specificity 63 %) and for ASL-rCBF 3.4 (sensitivity 75 %, specificity 60 %) (Table 5).

Kaplan-Meier analysis for TTR indicated that patients with rCBF and rCBV perfusion estimates below the calculated cut-off values had longer TTR than patients with higher perfusion values (Table 5). However, this was statistically significant for the DSC-rCBV parameter only. The Kaplan-Meier curves for DSC-rCBV, DSC-rCBF and ASL-rCBF are shown in Figure 10.

Table 5: ROC analysis and median TTR of single perfusion parameters
Area under the curve (AUC) (including p-value) and cut-off values with the highest Youden index of receiver operating characteristic (ROC) analysis, sensitivity and specificity referring to prediction of tumour recurrence are shown for each examined perfusion-related parameter. Namely rCBV and rCBF of DSC imaging and ASL-rCBF. The time to recurrence (TTR) (median, in days) (including the p-value of the log-rank test) after patient stratification according to the cut-off values is also demonstrated. The statistically significant values are indicated in bold. (30)

	AUC	Cut-off value	Sensitivity [%]	Specificity [%]	TTR [days]	p-value (log-rank test)
DSC-rCBV	0.71 **(p=0.006)**	≤ 6.8 > 6.8	73	64	510 225	**0.002**
DSC-rCBF	0.59 (p>0.05)	≤ 5.7 > 5.7	75	63	445 294	0.09
ASL-rCBF	0.58 (p>0.05)	≤ 3.4 > 3.4	75	60	368 310	0.10

Table 6: Areas under the curve (AUCs) of combined perfusion parameters.
AUCs were generated out of binary logistic regression of different perfusion-related parameters: DSC-rCBV and leakage, DSC-rCBF and ASL-rCBF. No p-value can be given since no cut-off can be determined out of probabilities.

Combined perfusion parameters	AUC
DSC-rCBV + ASL-rCBF	0.71
DSC-rCBV, DSC-rCBF + leakage	0.72
DSC-rCBV, DSC-rCBF, leakage + ASL-rCBF	0.74

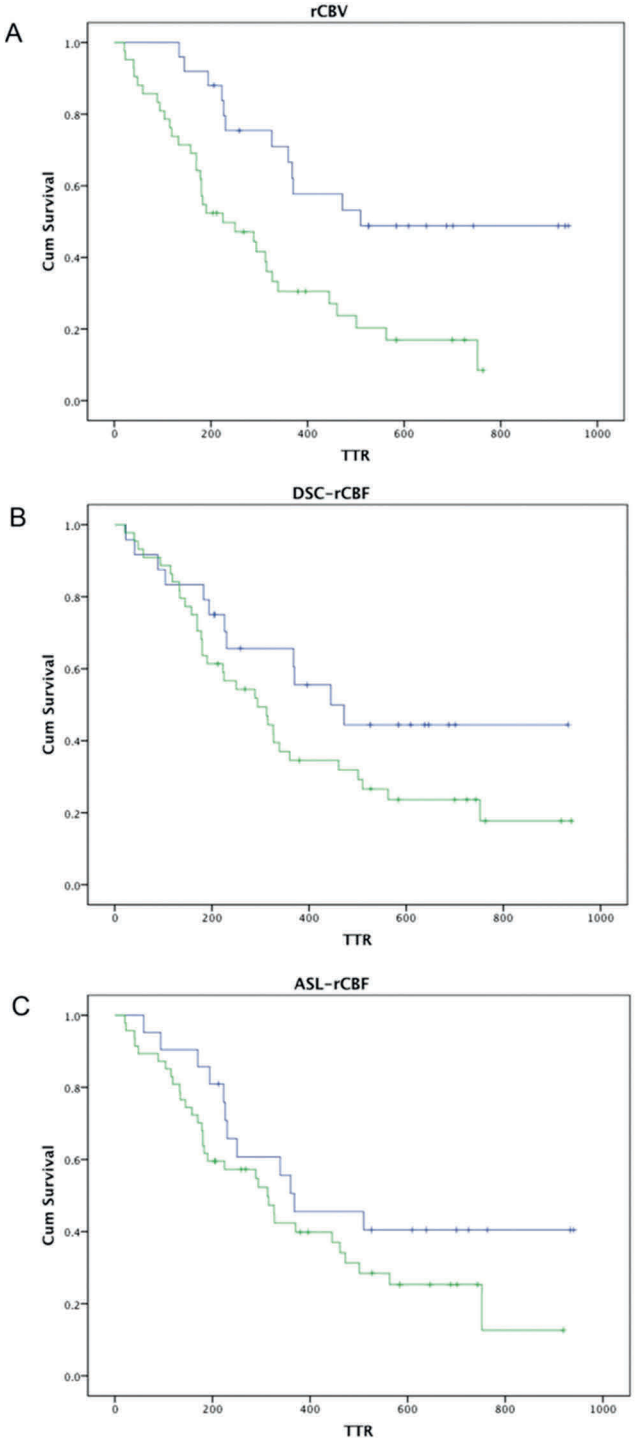

Figure 10: Kaplan-Meier survival curves for time to recurrence (TTR) in days for DSC-rCBV (A), DSC-rCBF (B) and ASL-rCBF (C). The blue lines represent TTR of patients with perfusion values below the perfusion thresholds shown in Table 5 while the green lines the TTR of patients with perfusion values above the threshold. The Kaplan-Meier survival curves are indicating that TTR is longer for patients with low tumour perfusion and shorter for patients with high perfusion estimates over the corresponding threshold (30).

4. Discussion

4.1 General considerations

Perfusion metrics and histopathological grading System

First this study confirms the prognostic value of perfusion metrics in general in patients with high grade gliomas compared to the already established WHO grading system. In previous studies histopathologic defined WHO grade has been shown to be the strongest predictor for overall survival in gliomas (7, 58, 59). Since rCBV refers to microvessel density (26, 60), which is also a histopathologic feature taking into account for conventional histopathologic grading, it was not surprising to find in this study that DSC-rCBV had a significant prognostic value, this being in accordance with other studies (24, 25, 61-64). However, these studies did not agree, whether rCBV is a grade-independent prognostic factor (25, 61, 62, 64) or merely a surrogate for histopathology. In order to exclude any bias and the possible impact of histopathologic grade on the elaborated prognostic model, the study was confined only to high-grade gliomas (WHO grade 3-4).Since this study showed significant differences in TTR among patients with tumours of the same histopathological grade, rCBV seems to be not only another independent surrogate for prognosis; it even seems to provide complementary information to the current WHO classification system as prognosticator.

The current glioma classification is based on the 2007 World Health Organization grading system, which is based from cytological characteristics of the tumours. Histopathologic grading however has some well-known limitations:

1) Grading can be inaccurate because of inter- and intraobserver variability (36). Due to the heterogeneity of high-grade tumours (52, 65), which are frequently incompletely resected, it is difficult to assign a tumour to a class. New studies have shown that molecular and cytogenetic features of a tumour yield promising information to improve the classification of gliomas

(66, 67). Eckel-Passow et al. classified gliomas into five groups based on three tumour markers: 1p/19q codeletion, IDH1/IDH2 mutation and promoter mutation of telomerase reverse transcriptase (TERT). These groups showed characteristic distributions of age at diagnosis and clinical behaviour (67). Even though histopathological grade represents an independent factor, molecular classification describes glioma variants in a better way, as stated by Ellison (66).

2) Not the whole tumour can be examined, especially if the tissue is gained through biopsy.

For these reasons, histopathology may have limited value in predicting tumour aggressiveness, prognosis and response to therapy. Both limitations can be overcomed by perfusion metrics:

First, perfusion parameters provide similar to molecular and cytogenetic features also insight into the functional tumour characteristics and may be a useful complement to any upcoming molecular/cytogenetic tumour classification system. For instance, rCBV refers both to microvessel and indirectly to cell density (26, 60). Therefore, it is typically elevated in aggressive tumours (and tumour parts) where cell division rate is high and neovascularization is in progress.

Also, to reduce sampling error, stereotactic biopsy could be guided by perfusion imaging (68). The method has been established in previous studies and implemented in many centres around the world (26). But to be fair, even if a biopsy is based on either rCBV or rCBF maps, it is possibly associated with sampling errors and result in biased information. In this study hot spots for DSC-rCBV and DSC-rCBF maps showed invariably the same spatially distribution. Former researchers concluded that vessel density (rCBV) does not necessarily correspond with high perfusion (rCBF) and both parameters should most likely provide different aspects of glioma pathophysiology (69). In fact, spatial distribution of DSC-rCBF and ASL-rCBF maps differed in most of the cases (N = 29) and was only in 9 cases identical.

Perfusion and corresponding microvessel properties

The cardinal role of blood perfusion-related biomarkers, such as DSC-rCBF or ASL-rCBF, in estimating the success of therapy is based on the assumption that low perfusion lowers the amount of drugs reaching the tumour bed and causes hypoxia, which in turn hampers the tumour response to radiotherapy (43) and leads to shorter TTR. As a matter of fact, perfusion MRI with non-invasive whole tumour sampling *in vivo* may stratify patients for different treatment regimens according to the estimated prognosis. In previous years, research in this promising field demonstrated prognostic relevance for both DSC- and ASL (25, 61, 70). One shortcoming of DSC-rCBF measurements may be attributed to an underestimation of tumour aggressiveness due to presence of immature tumour vessels with very slim lumina having no significant blood flow (71, 72). This postulation however would also affect DSC-rCBV metrics since DSC-rCBV reflects the amount of contrast passing through the capillary network, a phenomenon that is also dependant on functional, mature blood vessels since it is blood flow-related (60). It seems possible that DSC-rCBV relies to mature microvessels which often have dilated lumina, hence higher rCBV, which go along with low DSC-rCBF according to Hagen–Poiseuille equation (69, 71). Moreover, DSC-rCBF might also be decreased in high-grade, leaky tumours, since the accompanied interstitial hypertension leads to compression of the tumour vessels and subsequently decreases of blood flow (73). Most likely, a combination of the aforementioned pathophysiological phenomena may be the reason of the low predictive and prognostic value of DSC-rCBF measurements compared to the DSC-rCBV ones.

Prognostic value of ASL-rCBF in literature

ASL has been postulated to be an alternative to DSC MRI providing similar and highly correlated (i.e. linear regression coefficient, $R = 0.83$; $P < 0.005$) CBF values (27, 28, 31, 42, 43). Regarding the prognosis, ASL has been proved to be able to distinguish between high- and low-grade gliomas (28, 40). In addition absolute tumour blood flow acquired by ASL has been recognized as a

prognostic marker for TTR (70). Clinically, ASL provides an additional value to DSC imaging in differentiating pseudoprogression from early tumour progression (74) and in differentiating recurrent high-grade gliomas from stable disease (75). Nevertheless, there are several disadvantages of the ASL technique, which could explain the inferiority of ASL to DSC imaging in predicting the patient's prognosis:

1) The aforementioned poor SNR makes it difficult to place accurately the ROI;
2) The sensitivity of ASL to post labelling delay results in either underestimation of blood flow or in erroneous inclusion of large vessels in the tumour ROI;
3) The distribution of a diffusible tracer, like magnetically labelled water, across capillary membranes is not completely free and diffusion restrictions may apply (76, 77).

Besides the dependency of the perfusion signal on the inversion time, long arterial transit times could lead to differences between ASL- and DSC-based rCBF. Both normal or demyelinated white matter and tortuous tumour vasculature hold long transit times and may lead to underestimation of perfusion. Finally, the current computation of ASL does not provide CBV as perfusion-related parameter. But since it has been postulated that blood volume and blood flow provide different aspects of tumour perfusion both should be encountered in the survival analysis (78).

4.2 Correlations and comparison of DSC and ASL perfusion metrics

DSC-rCBF and DSC-rCBV maps showed the same spatial distribution of areas with the corresponding maximum perfusion values. This may be explained by the fact that DSC perfusion parameters are inherently dependent on each other, and was confirmed in lumped ROI analysis in other studies (79-81). On the other hand, hot spots of DSC-rCBF and ASL-rCBF differed. Moreover in contrast to previous reports (27, 28, 42) no significant correlation between ASL- and DSC-derived rCBF was found, though ASL-rCBF values did not

significantly differ from the DSC-rCBF estimates. As a matter of fact, although DSC- and ASL-rCBF values in this study are essentially concordant with those reported in literature (27, 55, 82) the lack of correlation could be attributed to the ROI placement and measurement strategy. Namely, in contrast to previous studies (27, 43), not the mean tumour rCBF value but the maximum value was used; the reference ROI was not placed like by Järnum et al. (27) in the cerebellum, but in the contralateral white matter. Interestingly, Lehmann et al. did not place the ROI around the whole tumour but placed two small ROIs within the tumour and averaged them (42). Finally, the patient cohorts between this study and similar ones in literature differed since other authors conducted their ASL measurements in heterogeneous tumour groups, including metastases as well as treated gliomas (27, 28). Notably, White et al. showed that positive linear, voxel-wise-based correlations between ASL- and DSC-rCBF can be observed in only 30-40 % of patients with brain neoplasms (43). Furthermore, the same authors demonstrated significant differences between ASL- and DSC-rCBF in both FLAIR-hyperintense and contrast-enhanced tumour regions, whereas Ludemann et al. stated that tumour perfusion values achieved by different techniques were not to be compared (83).

In addition to the lack of correlation between ASL- and DSC-derived rCBF results, the Bland-Altman plot pointed out that the difference between DSC-rCBF and ASL-rCBF increases with higher perfusion, which implies limited interchangeability/comparability of both perfusion techniques. There are very few Bland-Altman plots of DSC- and ASL-derived rCBF in literature, but similar tendencies for bias were observed in proportion to the rCBF values in the studies of Wong et al. in normal brain and of Järnum et al. in brain neoplasms (27, 31). One reason for the increasing difference between ASL- and DSC-derived rCBF in higher average values could be the susceptibility of ASL to arterial transit time. In that case, ASL-rCBF may appear lower than DSC-rCBF, like in this study (mean difference between DSC-rCBF and ASL-rCBF 1.47) and in other studies conducted in normal brain and brain tumours (27, 31, 43). Nevertheless, Warmuth et al. showed the opposite effect (28) highlighting the

dependence of the ASL on the transit times in different populations. To simplify this concept, we could assume that if the contralateral white matter is used as reference, the long transit time will underestimate the ASL-rCBF, and acting as denominator will result in artificially high tumour ASL-rCBF. This hypothesis challenges the appropriateness of contralateral white matter as reference region as well as the accuracy of measurements in low blood flow tumour areas (72). On the other hand, DSC remains relatively unaffected if delay-invariant circular deconvolution methods are applied in post-processing as done in the study presented here. Yet there is still uncertainty concerning the reproducibility of absolute quantification by ASL in presence of insufficient arterial function (e.g. carotid stenosis).

What should also be mentioned as reason for the lack of correlation and interchangeability between both CBF metrics are the different underlying physical properties and acquisition schemes applied. A characteristic example of distinct acquisition features between the techniques is the large vessel signal attenuation due to vascular crushers in ASL, which may increase the bias in highly vascularized tumours. A systematic bias may be also anchored in the underlying post-processing method of ASL. The tracer kinetic model (53), which assumes that brain tissue and blood are holding the same relaxation rate is as incorrect as the applied one-compartment Kety model to analyse arterial spin tagging data (84), which assumes that tagged water exchanges instantaneously across the blood brain barrier and is located predominantly in brain tissue. Thus, the ASL model used for this study gives rather a satisfactory approximation of the true perfusion in brain tissue (77). Finally, another reason for the lack of interchangeability/ comparability between the ASL- and DSC-based CBF is the different relaxation rates of the capillary and tissue spaces. Thereby, low cerebral blood flow values for example in white matter are slightly overestimated in ASL whereas high cerebral blood flows like in grey matter and tumour tissue are rather underestimated.

An interesting finding in this study was the difference in the spatial distribution of maximum rCBF values derived from DSC- and ASL imaging. The distribution of rCBF in DSC- and ASL-maps differed in the majority of cases (n = 29) and in only nine cases was the same. This underlines that ASL and DSC imaging provide different information about the tumour and it questions whether both techniques can be compared at all.

4.3 Prognostic value of DSC and ASL

Since the tumour aggressiveness is associated with its neovascularization, it was postulated that higher rCBV and rCBF values may indicate more aggressive tumours with shorter TTR. Weber et al. evaluated tumour response after treatment of metastases and showed that increase in tumour blood flow (perfusion) predicted tumour progression (41). According to Kaplan-Meier analysis in the present study, the DSC-rCBV results suited this hypothesis while a tendency was found for DSC-rCBF and ASL-rCBF. Although perfusion imaging by ASL may be correlated to vascular density (44) and DSC-rCBF was found to be significantly correlating with DSC-rCBV, both rCBF metrics failed to outperform the prognostic significance of DSC-rCBV. Nonetheless, both DSC-perfusion parameters and ASL-rCBF showed considerable unfavourable survival outcome in patients with highly-perfused, high-grade gliomas introducing mainly ASL-rCBF as a possible biomarker for predicting TTR considering the non-invasive nature of the technique, the sufficient SNR with newly launched sequences (27, 42), and the full coverage of the brain using newly introduced 3D ASL sequences (31).

4.4 Limitations

A distinct limitation of the study is the semi-quantitative estimation of ASL-rCBF using reference regions in the contralateral white matter. Though this is fair in terms of comparison with the DSC imaging, it cancels the inherent advantage of

quantification of rCBF by ASL. However, an advantage of the applied reference region approach is that the generated rCBF are somehow age-adjusted.

In studies that investigate the prognostic and diagnostic role of perfusion imaging one source of systematic bias could be due to the effect of glucocorticoid therapy on tumour perfusion. The present analysis did not include the possible effect of dexamethasone therapy as only few patients of our cohort were for a short period of time under glucocorticoid therapy. However, correlation with steroid dosing may be needed, although to date, technically rigorous reports looking at this subject have reached conflicting conclusions as to whether high-dose steroid administration acutely reduces rCBV in addition to its undisputed effect on permeability (57, 85, 86). This controversy will not be trivial to resolve definitively because alteration in permeability has a significant effect on the calculation of rCBV. Notably, it has been observed that dexamethasone caused no significant changes in rCBF (85).

4.5 Future endeavours

Future endeavours investigating brain tumours by ASL may profit from pseudocontinuous instead of pulsed ASL, since pseudocontinuous ASL provides higher SNR and reduced magnetization transfer effects (87). To overcome the underestimation of CBF in reference tissue (usually contralateral normal appearing white matter) with prolonged transit time, multiple post-labelling delay values can be used in both pulsed and pseudocontinuous ASL (88). This would also allow an accurate measurement of CBF in tumours with heterogeneous blood transit times. This method, however, adds complexity and expenditure of time in the post-processing and has neither been optimized nor tested for durability in the tumour imaging clinical practice. Vascular crushing gradients should optimally remain a user-controlled option and future studies in tumours may show their potential value or pitfalls in brain tumours staging (87). Finally, segmented 3D readouts with background suppression seem to enhance the diagnostic quality of ASL (87).

Regarding ASL post-processing, future studies may also aim at validating these preliminary results by using pseudocontinuous ASL and calculating tumour CBF after grey-white matter segmentation and normalization to healthy white matter (70). Simultaneously, any sequence optimization, i.e. as optimisation of the inversion time (89) would be useful. Finally, the measurement of arterial blood volume from ASL may also prove interesting regarding its predictive value (90). One drawback of DSC-imaging in this study was the semi-quantification of the derived parameters. Future endeavours investigating the comparability of ASL and DSC-imaging may pursue absolute quantification of DSC-rCBF. Any inaccuracy in the quantification of DSC-imaging could be improved by calibrating the CBV, calculated by standard DSC imaging, with an AIF-independent steady-state measurement of CBV (29).

4.6 Conclusion

This study confirms the prognostic value of “stand-alone” DSC- rCBV and highlights the comparable, though non-significant prognostic value of ASL- and DSC-rCBF estimations for prediction of tumour recurrence and assessment of TTR in patients with high-grade gliomas. The clear trend of ASL-rCBF measurements to identify patients with favourable outcome among those with high-grade gliomas can be further validated in future trials bearing in mind that ASL is a well-tolerated non-invasive technique. Furthermore, the implementation of ASL-rCBF results increased the prognostic power of DSC-technique thus, implying that ASL in the routine baseline imaging of gliomas may be advantageous for predicting time to adverse events like recurrence which, in turn, provide indices for the tumour aggressiveness and may have therapeutic implications for the patients, especially in therapy tailored regimens.

The lack of correlation and interchangeability between the DSC-rCBF and ASL-rCBF estimations with proportional bias in highly vascularized tumours might reflect the different underlying physical properties and data acquisition steps applied. It also underlines the need to prospectively analyse the tumour microenvironment by further rigorous voxel-based comparison and assessment of the spatial distribution pattern between the two techniques.

5. Abstract

5.1 Background and Purpose

Several studies have examined the predictive value of dynamic susceptibility contrast-enhanced (DSC) imaging and arterial spin labelling (ASL) in relation to histological grade, but less is known about their significance in terms of disease prognosis. Since ASL is gaining in importance, the purpose of this study was to evaluate the predictive value of both MRI techniques in assessing time to recurrence (TTR) in patients with high-grade gliomas and to examine for any interchangeability between them.

5.2 Materials and Methods

Sixty-nine cases of WHO Grade 3–4 gliomas underwent both DSC and ASL MRI. Normalized ASL and DSC-based perfusion maps were analysed yielding mean and maximum values for relative cerebral blood volume (rCBV), relative cerebral blood flow (rCBF), leakage and ASL blood flow estimates. Maps were compared regarding the spatial distribution of maximum DSC-rCBV, DSC-rCBF and ASL-rCBF. Wilcoxon test and Bland Altman plot analysis were applied to compare DSC-rCBF and ASL-rCBF. Spearman's rank correlation coefficient was determined for all perfusion parameters. Receiver operating characteristic curve analysis was applied to define the optimal cut-off of perfusion values for TTR. Survival curves were calculated by using the Kaplan-Meier method with log-rank test.

5.3 Results

The median values of ASL-rCBF, DSC-rCBF, and DSC-rCBV were 5.3, 6.9, and 8.0, respectively. Spearman's rank correlation showed significant correlation between the DSC parameters. There was neither significant correlation nor difference between ASL-rCBF and DSC-rCBF. Proportional bias was

demonstrated in the Bland-Altman plot analysis of ASL-rCBF and DSC-rCBF values. In ROC analysis, rCBV outperformed other parameters as prognostic factor (area under curve (AUC) = 0.71). DSC-rCBF was slightly superior to ASL-rCBF (AUC = 0.59 vs. 0.58). The combination of rCBV and ASL-rCBF (AUC = 0.71) was even to standalone rCBV. The best predictive value was achieved by combination of DSC-rCBV, DSC-rCBF, leakage and ASL-rCBF (AUC = 0.74). Unlikely to DSC-rCBV, DSC- and ASL-based rCBF parameters demonstrated moderate sensitivity and specificity for tumour recurrence with no statistically significant prognostic values in the survival analysis.

5.4 Conclusions

There was neither correlation nor interchangeability between the DSC-rCBF and ASL-rCBF estimations, which demonstrated comparable, though not significant prognostic value for TTR. On contrary, rCBV measurements provided the best available sensitivity and specificity to predict tumour recurrence and survival time in these patients. Combination of DSC- and ASL-perfusion metrics showed encouraging results for increasing the prognostic value of each ”stand-alone” technique.

6. References

1. Louis, D. N., Ohgaki, H., Wiestler, O. D., Cavenee, W. K., Burger, P. C., Jouvet, A., Scheithauer, B. W. and Kleihues, P. (2007) *The 2007 WHO classification of tumours of the central nervous system*. *Acta Neuropathol.* 114(2):97-109. (10.1007/s00401-007-0243-4)

2. Laperriere, N., Zuraw, L. and Cairncross, G. (2002) *Radiotherapy for newly diagnosed malignant glioma in adults: a systematic review*. *Radiotherapy and Oncology.* 64(3):259-273. (10.1016/S0167-8140(02)00078-6)

3. Stupp, R., Mason, W. P., van den Bent, M. J., Weller, M., Fisher, B., Taphoorn, M. J., Belanger, K., Brandes, A. A., Marosi, C., Bogdahn, U., Curschmann, J., Janzer, R. C., Ludwin, S. K., Gorlia, T., Allgeier, A., Lacombe, D., Cairncross, J. G., Eisenhauer, E. and Mirimanoff, R. O. (2005) *Radiotherapy plus concomitant and adjuvant temozolomide for glioblastoma*. *N Engl J Med.* 352(10):987-96. (10.1056/NEJMoa043330)

4. van den Bent, M. J. and Kros, J. M. (2007) *Predictive and prognostic markers in neuro-oncology*. *Journal of neuropathology and experimental neurology.* 66(12). (10.1097/nen.0b013e31815c39f1)

5. Nutt, C. L., Mani, D. R., Betensky, R. A., Tamayo, P., Cairncross, J. G., Ladd, C., Pohl, U., Hartmann, C., McLaughlin, M. E., Batchelor, T. T., Black, P. M., von Deimling, A., Pomeroy, S. L., Golub, T. R. and Louis, D. N. (2003) *Gene expression-based classification of malignant gliomas correlates better with survival than histological classification*. *Cancer Res.* 63(7):1602-7.

6. Walid, M. S. (2008) *Prognostic Factors for Long-Term Survival after Glioblastoma*. *Perm J.* 12(4):45-8.

7. Bauman, G., Lote, K., Larson, D., Stalpers, L., Leighton, C., Fisher, B., Wara, W., MacDonald, D., Stitt, L. and Cairncross, J. G. (1999) *Pretreatment factors predict overall survival for patients with low-grade glioma: a recursive partitioning analysis*. *Int J Radiat Oncol Biol Phys.* 45(4):923-9.

8. Shaw, E., Arusell, R., Scheithauer, B., O'Fallon, J., O'Neill, B., Dinapoli, R., Nelson, D., Earle, J., Jones, C., Cascino, T., Nichols, D., Ivnik, R., Hellman, R., Curran, W. and Abrams, R. (2002) *Prospective randomized trial of low- versus high-dose radiation therapy in adults with supratentorial low-grade glioma: initial report of a North Central Cancer Treatment Group/Radiation Therapy Oncology Group/Eastern Cooperative Oncology Group study*. *J Clin Oncol.* 20(9):2267-76.

9. Gorlia, T., van den Bent, M. J., Hegi, M. E., Mirimanoff, R. O., Weller, M., Cairncross, J. G., Eisenhauer, E., Belanger, K., Brandes, A. A., Allgeier, A., Lacombe, D. and Stupp, R. (2008) *Nomograms for predicting survival of patients with newly diagnosed glioblastoma: prognostic factor analysis of EORTC and NCIC trial 26981-22981/CE.3*. *Lancet Oncol.* 9(1):29-38. (10.1016/s1470-2045(07)70384-4)

10. Ostrom, Q. T., Gittleman, H., Xu, J., Kromer, C., Wolinsky, Y., Kruchko, C. and Barnholtz-Sloan, J. S. (2016) *CBTRUS Statistical Report: Primary Brain and Other Central Nervous System Tumors Diagnosed in the United States in 2009–2013*. *Neuro-Oncology.* 18(suppl 5):v1-v75. (10.1093/neuonc/now207)

11. Sun, T., Warrington, N. M., Luo, J., Brooks, M. D., Dahiya, S., Snyder, S. C., Sengupta, R. and Rubin, J. B. (2014) *Sexually dimorphic RB inactivation underlies mesenchymal glioblastoma prevalence in males*. *J Clin Invest.* 124(9):4123-33. (10.1172/jci71048)

12. Hegi, M. E., Diserens, A. C., Gorlia, T., Hamou, M. F., de Tribolet, N., Weller, M., Kros, J. M., Hainfellner, J. A., Mason, W., Mariani, L., Bromberg, J. E., Hau, P., Mirimanoff, R. O., Cairncross, J. G., Janzer, R. C. and Stupp, R. (2005) *MGMT gene silencing and benefit from temozolomide in glioblastoma*. *N Engl J Med.* 352(10):997-1003. (10.1056/NEJMoa043331)

13. Hung, K. S. and Howng, S. L. (2003) *Prognostic significance of annexin VII expression in glioblastomas multiforme in humans*. *J Neurosurg.* 99(5):886-92. (10.3171/jns.2003.99.5.0886)

14. Ulutin, C., Fayda, M., Aksu, G., Cetinayak, O., Kuzhan, O., Ors, F. and Beyzadeoglu, M. (2006) *Primary glioblastoma multiforme in younger patients: a single-institution experience*. *Tumori.* 92(5):407-11.

15. Osoba, D., Brada, M., Prados, M. D. and Yung, W. K. (2000) *Effect of disease burden on health-related quality of life in patients with malignant gliomas*. *Neuro Oncol.* 2(4):221-8.

16. Lupien, S. J., Gillin, C. J. and Hauger, R. L. (1999) *Working memory is more sensitive than declarative memory to the acute effects of corticosteroids: a dose-response study in humans*. *Behav Neurosci.* 113(3):420-30.

17. Young, A. H., Sahakian, B. J., Robbins, T. W. and Cowen, P. J. (1999) *The effects of chronic administration of hydrocortisone on cognitive function in normal male volunteers*. *Psychopharmacology (Berl).* 145(3):260-6.

18. Heimans, J. J. and Taphoorn, M. J. (2002) *Impact of brain tumour treatment on quality of life*. *J Neurol.* 249(8):955-60. (10.1007/s00415-002-0839-5)

19. Liu, R., Page, M., Solheim, K., Fox, S. and Chang, S. M. (2009) *Quality of life in adults with brain tumors: Current knowledge and future directions*. *Neuro-Oncology.* 11(3):330-339. (10.1215/15228517-2008-093)

20. Meyers, C. A. and Hess, K. R. (2003) *Multifaceted end points in brain tumor clinical trials: cognitive deterioration precedes MRI progression*. *Neuro Oncol.* 5(2):89-95. (10.1215/s1522-8517-02-00026-1)

21. van den Bent, M. (2007) *Astrocytic Tumors*. In: J. M. P. Joachim M. Baehring, ed. *Brain Tumors Practical Guide to Diagnosis and Treatment*. New York, London: Informa Healthcare USA, Inc.:159-192.

22. Law, M., Young, R., Babb, J., Rad, M., Sasaki, T., Zagzag, D. and Johnson, G. (2006) *Comparing perfusion metrics obtained from a single compartment versus pharmacokinetic modeling methods using dynamic susceptibility contrast-enhanced perfusion MR imaging with glioma grade*. *AJNR Am J Neuroradiol.* 27(9):1975-82.

23. Law, M., Yang, S., Babb, J. S., Knopp, E. A., Golfinos, J. G., Zagzag, D. and Johnson, G. (2004) *Comparison of cerebral blood volume and vascular permeability from dynamic susceptibility contrast-enhanced perfusion MR imaging with glioma grade*. *AJNR Am J Neuroradiol.* 25(5):746-55.

24. Law, M., Oh, S., Babb, J. S., Wang, E., Inglese, M., Zagzag, D., Knopp, E. A. and Johnson, G. (2006) *Low-grade gliomas: dynamic susceptibility-weighted contrast-enhanced perfusion MR imaging--prediction of patient clinical response*. *Radiology.* 238(2):658-67. (10.1148/radiol.2382042180)

25. Bisdas, S., Kirkpatrick, M., Giglio, P., Welsh, C., Spampinato, M. V. and Rumboldt, Z. (2009) *Cerebral blood volume measurements by perfusion-weighted MR imaging in gliomas: ready for prime time in predicting short-term outcome and recurrent disease? AJNR Am J Neuroradiol.* 30(4):681-8. (10.3174/ajnr.A1465)

26. Cha, S., Knopp, E. A., Johnson, G., Wetzel, S. G., Litt, A. W. and Zagzag, D. (2002) *Intracranial mass lesions: dynamic contrast-enhanced susceptibility-weighted echo-planar perfusion MR imaging*. *Radiology.* 223(1). (10.1148/radiol.2231010594)

27. Jarnum, H., Steffensen, E. G., Knutsson, L., Frund, E. T., Simonsen, C. W., Lundbye-Christensen, S., Shankaranarayanan, A., Alsop, D. C.,

Jensen, F. T. and Larsson, E. M. (2010) *Perfusion MRI of brain tumours: a comparative study of pseudo-continuous arterial spin labelling and dynamic susceptibility contrast imaging*. *Neuroradiology.* 52(4):307-17. (10.1007/s00234-009-0616-6)

28. Warmuth, C., Gunther, M. and Zimmer, C. (2003) *Quantification of blood flow in brain tumors: comparison of arterial spin labeling and dynamic susceptibility-weighted contrast-enhanced MR imaging*. *Radiology.* 228(2):523-32. (10.1148/radiol.2282020409)

29. Sakaie, K. E., Shin, W., Curtin, K. R., McCarthy, R. M., Cashen, T. A. and Carroll, T. J. (2005) *Method for improving the accuracy of quantitative cerebral perfusion imaging*. *J Magn Reson Imaging.* 21(5):512-9. (10.1002/jmri.20305)

30. Rau, M. K., Braun, C., Skardelly, M., Schittenhelm, J., Paulsen, F., Bender, B., Ernemann, U. and Bisdas, S. (2014) *Prognostic value of blood flow estimated by arterial spin labeling and dynamic susceptibility contrast-enhanced MR imaging in high-grade gliomas*. *J Neurooncol.* 120(3):557-66. (10.1007/s11060-014-1586-z)

31. Wong, A. M., Yan, F. X. and Liu, H. L. (2014) *Comparison of three-dimensional pseudo-continuous arterial spin labeling perfusion imaging with gradient-echo and spin-echo dynamic susceptibility contrast MRI*. *J Magn Reson Imaging.* 39(2):427-33. (10.1002/jmri.24178)

32. Boxerman, J. L., Hamberg, L. M., Rosen, B. R. and Weisskoff, R. M. (1995) *MR contrast due to intravascular magnetic susceptibility perturbations*. *Magn Reson Med.* 34(4):555-66.

33. Kennan, R. P., Zhong, J. and Gore, J. C. (1994) *Intravascular susceptibility contrast mechanisms in tissues*. *Magn Reson Med.* 31(1):9-21.

34. Provenzale, J. M., Mukundan, S. and Barboriak, D. P. (2006) *Diffusion-weighted and Perfusion MR Imaging for Brain Tumor Characterization and Assessment of Treatment Response1*. *Radiology.* 239(3):632-649. (10.1148/radiol.2393042031)

35. Sadowski, E. A., Bennett, L. K., Chan, M. R., Wentland, A. L., Garrett, A. L., Garrett, R. W. and Djamali, A. (2007) *Nephrogenic Systemic Fibrosis: Risk Factors and Incidence Estimation1*. *Radiology.* 243(1):148-157. (10.1148/radiol.2431062144)

36. Jackson, R. J., Fuller, G. N., Abi-Said, D., Lang, F. F., Gokaslan, Z. L., Shi, W. M., Wildrick, D. M. and Sawaya, R. (2001) *Limitations of stereotactic biopsy in the initial management of gliomas*. *Neuro-oncology.* 3(3). (10.1215/15228517-3-3-193)

37. Zaharchuk, G. (2007) *Theoretical basis of hemodynamic MR imaging techniques to measure cerebral blood volume, cerebral blood flow, and permeability*. *AJNR Am J Neuroradiol.* 28(10):1850-8. (10.3174/ajnr.A0831)

38. Lu, H., Clingman, C., Golay, X. and van Zijl, P. C. (2004) *Determining the longitudinal relaxation time (T1) of blood at 3.0 Tesla*. *Magn Reson Med.* 52(3):679-82. (10.1002/mrm.20178)

39. Koziak, A. M., Winter, J., Lee, T. Y., Thompson, R. T. and St Lawrence, K. S. (2008) *Validation study of a pulsed arterial spin labeling technique by comparison to perfusion computed tomography*. *Magn Reson Imaging.* 26(4):543-53. (10.1016/j.mri.2007.10.005)

40. Furtner, J., Schopf, V., Schewzow, K., Kasprian, G., Weber, M., Woitek, R., Asenbaum, U., Preusser, M., Marosi, C., Hainfellner, J. A., Widhalm, G., Wolfsberger, S. and Prayer, D. (2014) *Arterial spin-labeling assessment of normalized vascular intratumoral signal intensity as a predictor of histologic grade of astrocytic neoplasms*. *AJNR Am J Neuroradiol.* 35(3):482-9. (10.3174/ajnr.A3705)

41. Weber, M. A., Gunther, M., Lichy, M. P., Delorme, S., Bongers, A., Thilmann, C., Essig, M., Zuna, I., Schad, L. R., Debus, J. and Schlemmer, H. P. (2003) *Comparison of arterial spin-labeling techniques and dynamic susceptibility-weighted contrast-enhanced MRI in perfusion imaging of normal brain tissue*. *Invest Radiol.* 38(11):712-8. (10.1097/01.rli.0000084890.57197.54)

42. Lehmann, P., Monet, P., de Marco, G., Saliou, G., Perrin, M., Stoquart-Elsankari, S., Bruniau, A. and Vallee, J. N. (2010) *A comparative study of perfusion measurement in brain tumours at 3 Tesla MR: Arterial spin labeling versus dynamic susceptibility contrast-enhanced MRI*. *Eur Neurol.* 64(1):21-6. (10.1159/000311520)

43. White, C. M., Pope, W. B., Zaw, T., Qiao, J., Naeini, K. M., Lai, A., Nghiemphu, P. L., Wang, J. J., Cloughesy, T. F. and Ellingson, B. M. (2014) *Regional and Voxel-Wise Comparisons of Blood Flow Measurements Between Dynamic Susceptibility Contrast Magnetic Resonance Imaging (DSC-MRI) and Arterial Spin Labeling (ASL) in Brain Tumors*. *J Neuroimaging.* 24(1):23-30. (10.1111/j.1552-6569.2012.00703.x)

44. Noguchi, T., Yoshiura, T., Hiwatashi, A., Togao, O., Yamashita, K., Nagao, E., Shono, T., Mizoguchi, M., Nagata, S., Sasaki, T., Suzuki, S. O., Iwaki, T., Kobayashi, K., Mihara, F. and Honda, H. (2008) *Perfusion Imaging of Brain Tumors Using Arterial Spin-Labeling: Correlation with Histopathologic Vascular Density*. *American Journal of Neuroradiology.* 29(4):688-693. (10.3174/ajnr.A0903)

45. Wong, E. C., Buxton, R. B. and Frank, L. R. (1998) *Quantitative imaging of perfusion using a single subtraction (QUIPSS and QUIPSS II)*. *Magnetic resonance in medicine : official journal of the Society of Magnetic Resonance in Medicine / Society of Magnetic Resonance in Medicine.* 39(5). (10.1002/mrm.1910390506)

46. Wong, E. C., Buxton, R. B. and Frank, L. R. (1997) *Implementation of quantitative perfusion imaging techniques for functional brain mapping using pulsed arterial spin labeling*. *NMR Biomed.* 10(4-5):237-49.

47. Tan, H., Maldjian, J. A., Pollock, J. M., Burdette, J. H., Yang, L. Y., Deibler, A. R. and Kraft, R. A. (2009) *A fast, effective filtering method for improving clinical pulsed arterial spin labeling MRI*. *J Magn Reson Imaging.* 29(5):1134-9. (10.1002/jmri.21721)

48. Paulson, E. S. and Schmainda, K. M. (2008) *Comparison of Dynamic Susceptibility-weighted Contrast-enhanced MR Methods: Recommendations for Measuring Relative Cerebral Blood Volume in Brain Tumors1*. *Radiology.* 249(2):601-613. (10.1148/radiol.2492071659)

49. Boxerman, J. L., Schmainda, K. M. and Weisskoff, R. M. (2006) *Relative cerebral blood volume maps corrected for contrast agent extravasation significantly correlate with glioma tumor grade, whereas uncorrected maps do not*. *AJNR Am J Neuroradiol.* 27(4):859-67.

50. Ye, F. Q., Berman, K. F., Ellmore, T., Esposito, G., van Horn, J. D., Yang, Y., Duyn, J., Smith, A. M., Frank, J. A., Weinberger, D. R. and McLaughlin, A. C. (2000) *H(2)(15)O PET validation of steady-state arterial spin tagging cerebral blood flow measurements in humans*. *Magn Reson Med.* 44(3):450-6.

51. Koh, T. S., Bisdas, S., Koh, D. M. and Thng, C. H. (2011) *Fundamentals of tracer kinetics for dynamic contrast-enhanced MRI*. *J Magn Reson Imaging.* 34(6):1262-76. (10.1002/jmri.22795)

52. Stecco, A., Pisani, C., Quarta, R., Brambilla, M., Masini, L., Beldi, D., Zizzari, S., Fossaceca, R., Krengli, M. and Carriero, A. (2011) *DTI and PWI analysis of peri-enhancing tumoral brain tissue in patients treated for glioblastoma*. *J Neurooncol.* 102(2):261-71. (10.1007/s11060-010-0310-x)

53. Buxton, R. B., Frank, L. R., Wong, E. C., Siewert, B., Warach, S. and Edelman, R. R. (1998) *A general kinetic model for quantitative perfusion imaging with arterial spin labeling*. *Magn Reson Med.* 40(3):383-96.

54. Wetzel, S. G., Cha, S., Johnson, G., Lee, P., Law, M., Kasow, D. L., Pierce, S. D. and Xue, X. (2002) *Relative cerebral blood volume*

measurements in intracranial mass lesions: interobserver and intraobserver reproducibility study. *Radiology.* 224(3):797-803.

55. Hirai, T., Kitajima, M., Nakamura, H., Okuda, T., Sasao, A., Shigematsu, Y., Utsunomiya, D., Oda, S., Uetani, H., Morioka, M. and Yamashita, Y. (2011) *Quantitative blood flow measurements in gliomas using arterial spin-labeling at 3T: intermodality agreement and inter- and intraobserver reproducibility study*. *AJNR Am J Neuroradiol.* 32(11):2073-9. (10.3174/ajnr.A2725)

56. Thomsen, H. S., Muller, R. N., Mattrey, R. F. and Agati, R. (1999) *Trends in contrast media.* Berlin ; New York: Springer.

57. Bastin, M. E., Carpenter, T. K., Armitage, P. A., Sinha, S., Wardlaw, J. M. and Whittle, I. R. (2006) *Effects of dexamethasone on cerebral perfusion and water diffusion in patients with high-grade glioma*. *AJNR Am J Neuroradiol.* 27(2):402-8.

58. Pignatti, F., van den Bent, M., Curran, D., Debruyne, C., Sylvester, R., Therasse, P., Afra, D., Cornu, P., Bolla, M., Vecht, C. and Karim, A. B. (2002) *Prognostic factors for survival in adult patients with cerebral low-grade glioma*. *J Clin Oncol.* 20(8):2076-84.

59. Scott, C. B., Scarantino, C., Urtasun, R., Movsas, B., Jones, C. U., Simpson, J. R., Fischbach, A. J. and Curran, W. J., Jr. (1998) *Validation and predictive power of Radiation Therapy Oncology Group (RTOG) recursive partitioning analysis classes for malignant glioma patients: a report using RTOG 90-06*. *Int J Radiat Oncol Biol Phys.* 40(1):51-5.

60. Sadeghi, N., D'Haene, N., Decaestecker, C., Levivier, M., Metens, T., Maris, C., Wikler, D., Baleriaux, D., Salmon, I. and Goldman, S. (2008) *Apparent diffusion coefficient and cerebral blood volume in brain gliomas: relation to tumor cell density and tumor microvessel density based on stereotactic biopsies*. *AJNR Am J Neuroradiol.* 29(3):476-82. (10.3174/ajnr.A0851)

61. Hirai, T., Murakami, R., Nakamura, H., Kitajima, M., Fukuoka, H., Sasao, A., Akter, M., Hayashida, Y., Toya, R., Oya, N., Awai, K., Iyama, K., Kuratsu, J. I. and Yamashita, Y. (2008) *Prognostic value of perfusion MR imaging of high-grade astrocytomas: long-term follow-up study*. *AJNR Am J Neuroradiol.* 29(8):1505-10. (10.3174/ajnr.A1121)

62. Lev, M. H., Ozsunar, Y., Henson, J. W., Rasheed, A. A., Barest, G. D., Harsh, G. R. t., Fitzek, M. M., Chiocca, E. A., Rabinov, J. D., Csavoy, A. N., Rosen, B. R., Hochberg, F. H., Schaefer, P. W. and Gonzalez, R. G. (2004) *Glial tumor grading and outcome prediction using dynamic spin-echo MR susceptibility mapping compared with conventional contrast-*

enhanced MR: confounding effect of elevated rCBV of oligodendrogliomas [corrected]. *AJNR Am J Neuroradiol.* 25(2):214-21.

63. Law, M., Oh, S., Johnson, G., Babb, J. S., Zagzag, D., Golfinos, J. and Kelly, P. J. (2006) *Perfusion magnetic resonance imaging predicts patient outcome as an adjunct to histopathology: a second reference standard in the surgical and nonsurgical treatment of low-grade gliomas*. *Neurosurgery.* 58(6):1099-107; discussion 1099-107. (10.1227/01.neu.0000215944.81730.18)

64. Mills, S. J., Patankar, T. A., Haroon, H. A., Baleriaux, D., Swindell, R. and Jackson, A. (2006) *Do cerebral blood volume and contrast transfer coefficient predict prognosis in human glioma? AJNR Am J Neuroradiol.* 27(4):853-8.

65. Catalaa, I., Henry, R., Dillon, W. P., Graves, E. E., McKnight, T. R., Lu, Y., Vigneron, D. B. and Nelson, S. J. (2006) *Perfusion, diffusion and spectroscopy values in newly diagnosed cerebral gliomas*. *NMR Biomed.* 19(4):463-75. (10.1002/nbm.1059)

66. Ellison, D. W. (2015) *Multiple Molecular Data Sets and the Classification of Adult Diffuse Gliomas*. *N Engl J Med.* 372(26):2555-7. (10.1056/NEJMe1506813)

67. Eckel-Passow, J. E., Lachance, D. H., Molinaro, A. M., Walsh, K. M., Decker, P. A., Sicotte, H., Pekmezci, M., Rice, T., Kosel, M. L., Smirnov, I. V., Sarkar, G., Caron, A. A., Kollmeyer, T. M., Praska, C. E., Chada, A. R., Halder, C., Hansen, H. M., McCoy, L. S., Bracci, P. M., Marshall, R., Zheng, S., Reis, G. F., Pico, A. R., O'Neill, B. P., Buckner, J. C., Giannini, C., Huse, J. T., Perry, A., Tihan, T., Berger, M. S., Chang, S. M., Prados, M. D., Wiemels, J., Wiencke, J. K., Wrensch, M. R. and Jenkins, R. B. (2015) *Glioma Groups Based on 1p/19q, IDH, and TERT Promoter Mutations in Tumors*. *N Engl J Med.* 372(26):2499-508. (10.1056/NEJMoa1407279)

68. Knopp, E. A., Cha, S., Johnson, G., Mazumdar, A., Golfinos, J. G., Zagzag, D., Miller, D. C., Kelly, P. J. and Kricheff, I. I. (1999) *Glial Neoplasms: Dynamic Contrast-enhanced T2*-weighted MR Imaging1*. *Radiology.* 211(3):791-798.

69. Gillies, R. J., Schornack, P. A., Secomb, T. W. and Raghunand, N. (1999) *Causes and effects of heterogeneous perfusion in tumors*. *Neoplasia.* 1(3):197-207.

70. Furtner, J., Bender, B., Braun, C., Schittenhelm, J., Skardelly, M., Ernemann, U. and Bisdas, S. (2014) *Prognostic value of blood flow measurements using arterial spin labeling in gliomas*. *PLoS One.* 9(6):e99616. (10.1371/journal.pone.0099616)

71. Miyagami, M. and Katayama, Y. (2005) *Angiogenesis of glioma: evaluation of ultrastructural characteristics of microvessels and tubular bodies (Weibel-Palade) in endothelial cells and immunohistochemical findings with VEGF and p53 protein*. *Med Mol Morphol.* 38(1):36-42. (10.1007/s00795-004-0273-0)

72. Petersen, E. T., Zimine, I., Ho, Y. C. and Golay, X. (2006) *Non-invasive measurement of perfusion: a critical review of arterial spin labelling techniques*. *Br J Radiol.* 79(944):688-701. (10.1259/bjr/67705974)

73. Jain, R. K. (2005) *Normalization of tumor vasculature: an emerging concept in antiangiogenic therapy*. *Science.* 307(5706):58-62. (10.1126/science.1104819)

74. Choi, Y. J., Kim, H. S., Jahng, G. H., Kim, S. J. and Suh, D. C. (2013) *Pseudoprogression in patients with glioblastoma: added value of arterial spin labeling to dynamic susceptibility contrast perfusion MR imaging*. *Acta Radiol.* 54(4):448-54. (10.1177/0284185112474916)

75. Seeger, A., Braun, C., Skardelly, M., Paulsen, F., Schittenhelm, J., Ernemann, U. and Bisdas, S. (2013) *Comparison of three different MR perfusion techniques and MR spectroscopy for multiparametric assessment in distinguishing recurrent high-grade gliomas from stable disease*. *Acad Radiol.* 20(12):1557-65. (10.1016/j.acra.2013.09.003)

76. Eichling, J. O., Raichle, M. E., Grubb, R. L., Jr. and Ter-Pogossian, M. M. (1974) *Evidence of the limitations of water as a freely diffusible tracer in brain of the rhesus monkey*. *Circ Res.* 35(3):358-64.

77. St Lawrence, K. S., Frank, J. A. and McLaughlin, A. C. (2000) *Effect of restricted water exchange on cerebral blood flow values calculated with arterial spin tagging: a theoretical investigation*. *Magn Reson Med.* 44(3):440-9.

78. Moffat, B. A., Chen, M., Kariaapper, M. S., Hamstra, D. A., Hall, D. E., Stojanovska, J., Johnson, T. D., Blaivas, M., Kumar, M., Chenevert, T. L., Rehemtulla, A. and Ross, B. D. (2006) *Inhibition of vascular endothelial growth factor (VEGF)-A causes a paradoxical increase in tumor blood flow and up-regulation of VEGF-D*. *Clin Cancer Res.* 12(5):1525-32. (10.1158/1078-0432.ccr-05-1408)

79. Shin, J. H., Lee, H. K., Kwun, B. D., Kim, J. S., Kang, W., Choi, C. G. and Suh, D. C. (2002) *Using relative cerebral blood flow and volume to evaluate the histopathologic grade of cerebral gliomas: preliminary results*. *AJR Am J Roentgenol.* 179(3):783-9. (10.2214/ajr.179.3.1790783)

80. Hakyemez, B., Erdogan, C., Ercan, I., Ergin, N., Uysal, S. and Atahan, S. (2005) *High-grade and low-grade gliomas: differentiation by using perfusion MR imaging*. *Clin Radiol.* 60(4):493-502. (10.1016/j.crad.2004.09.009)

81. Thomsen, H., Steffensen, E. and Larsson, E. M. (2012) *Perfusion MRI (dynamic susceptibility contrast imaging) with different measurement approaches for the evaluation of blood flow and blood volume in human gliomas*. *Acta Radiol.* 53(1):95-101. (10.1258/ar.2011.110242)

82. Chawla, S., Wang, S., Wolf, R. L., Woo, J. H., Wang, J., O'Rourke, D. M., Judy, K. D., Grady, M. S., Melhem, E. R. and Poptani, H. (2007) *Arterial spin-labeling and MR spectroscopy in the differentiation of gliomas*. *AJNR Am J Neuroradiol.* 28(9):1683-9. (10.3174/ajnr.A0673)

83. Ludemann, L., Warmuth, C., Plotkin, M., Forschler, A., Gutberlet, M., Wust, P. and Amthauer, H. (2009) *Brain tumor perfusion: comparison of dynamic contrast enhanced magnetic resonance imaging using T1, T2, and T2* contrast, pulsed arterial spin labeling, and H2(15)O positron emission tomography*. *Eur J Radiol.* 70(3):465-74. (10.1016/j.ejrad.2008.02.012)

84. Kety, S. S. (1951) *The theory and applications of the exchange of inert gas at the lungs and tissues*. *Pharmacol Rev.* 3(1):1-41.

85. Ostergaard, L., Hochberg, F. H., Rabinov, J. D., Sorensen, A. G., Lev, M., Kim, L., Weisskoff, R. M., Gonzalez, R. G., Gyldensted, C. and Rosen, B. R. (1999) *Early changes measured by magnetic resonance imaging in cerebral blood flow, blood volume, and blood-brain barrier permeability following dexamethasone treatment in patients with brain tumors*. *J Neurosurg.* 90(2):300-5. (10.3171/jns.1999.90.2.0300)

86. Wilkinson, I. D., Jellineck, D. A., Levy, D., Giesel, F. L., Romanowski, C. A., Miller, B. A. and Griffiths, P. D. (2006) *Dexamethasone and enhancing solitary cerebral mass lesions: alterations in perfusion and blood-tumor barrier kinetics shown by magnetic resonance imaging*. *Neurosurgery.* 58(4):640-6; discussion 640-6. (10.1227/01.neu.0000204873.68395.a0)

87. Alsop, D. C., Detre, J. A., Golay, X., Gunther, M., Hendrikse, J., Hernandez-Garcia, L., Lu, H., MacIntosh, B. J., Parkes, L. M., Smits, M., van Osch, M. J., Wang, D. J., Wong, E. C. and Zaharchuk, G. (2015) *Recommended implementation of arterial spin-labeled perfusion MRI for clinical applications: A consensus of the ISMRM perfusion study group and the European consortium for ASL in dementia*. *Magn Reson Med.* 73(1):102-16. (10.1002/mrm.25197)

88. Macintosh, B. J., Marquardt, L., Schulz, U. G., Jezzard, P. and Rothwell, P. M. (2012) *Hemodynamic alterations in vertebrobasilar large artery disease assessed by arterial spin-labeling MR imaging*. *AJNR Am J Neuroradiol.* 33(10):1939-44. (10.3174/ajnr.A3090)

89. MacIntosh, B. J., Filippini, N., Chappell, M. A., Woolrich, M. W., Mackay, C. E. and Jezzard, P. (2010) *Assessment of arterial arrival times derived from multiple inversion time pulsed arterial spin labeling MRI*. *Magn Reson Med.* 63(3):641-7. (10.1002/mrm.22256)

90. van Westen, D., Petersen, E. T., Wirestam, R., Siemund, R., Bloch, K. M., Stahlberg, F., Bjorkman-Burtscher, I. M. and Knutsson, L. (2011) *Correlation between arterial blood volume obtained by arterial spin labelling and cerebral blood volume in intracranial tumours*. *MAGMA.* 24(4):211-23. (10.1007/s10334-011-0255-x)

7. German Abstract

Einleitung

Verschiedene Studien haben sich mit dem diagnostischen Wert der dynamischen kontrastmittel-unterstützten Suszeptibilitäts-gewichteten (dynamic susceptibility contrast enhanced, DSC) Bildgebung und der arteriellen Spinmarkierung (Arterial Spin Labelling, ASL) bei Gliomen in Bezug auf ihre histologische Klassifikation befasst. Über den prädiktiven Wert dieser Magnetresonanztomographie-Techniken hinsichtlich der Prognose der Patienten ist bisher jedoch weniger bekannt. Da die kontrastmittelfreie ASL-Bildgebung immer weiter an Bedeutung zunimmt, ist der Zweck dieser Studie, einerseits den prädiktiven Wert beider bildgebenden Methoden hinsichtlich der Vorhersage der rezidivfreien Überlebenszeit sowie andererseits deren Austauschbarkeit bei Patienten mit höhergradigen Gliomen zu untersuchen.

Material und Methoden

Insgesamt lagen von 69 WHO Grad 3-4 Gliomen die Rohdaten der DSC- und der ASL-Bildgebung vor. Die DSC- und ASL-basierten Perfusionskarten wurden ausgewertet und jeweils die mittleren und maximalen Werte des relativen zerebralen Blutvolumens (relative cerebral blood volume, rCBV), des relativen zerebralen Blutflusses (relative cerebral blood flow, rCBF) und des Kontrastmittel-Austritts in den Extravasalraum (leakage) erfasst. Die Perfusionskarten wurden hinsichtlich der räumlichen Verteilung der maximalen Perfusionswerte innerhalb des Tumors miteinander verglichen. Mittels Wilcoxon-Mann-Whitney-Test und Bland-Altman-Diagramm wurden DSC und ASL hinsichtlich rCBF miteinander verglichen. Der Rangkorrelationskoeffizient nach Spearman wurde für alle Perfusionsparameter bestimmt. Um den optimalen Schwellen-Perfusionswert zur Vorhersage des rezidivfreien Intervalls zu bestimmen, wurde eine Receiver Operating Characteristic (ROC)- Kurve

erstellt. Die Überlebenskurven wurden nach Kaplan-Meier mit dem Log-Rang-Test erstellt.

Ergebnisse

Der Median von ASL-rCBF, DSC-rCBF und DSC-rCBV lag bei 5,3; 6,9; bzw. 8,0. Die Rangkorrelation nach Spearman ergab für alle DSC-Perfusionsparameter eine signifikante Korrelation. Für ASL-rCBF und DSC-rCBF konnte weder eine signifikante Korrelation noch ein signifikanter Unterschied nachgewiesen werden (Wilcoxon-Mann-Whitney-Test p = 0,07). Im Bland-Altman-Diagramm zeigte sich eine leichte asymmetrische Verzerrung, so dass insbesondere bei höheren Durchschnittswerten keine Austauschbarkeit der DSC-rCBF- und ASL-rCBF-Werte vorlag. In der ROC-Analyse erzielte DSC-rCBV das beste Ergebnis als einzelstehender Prognosefaktor (Area under the curve, AUC = 0,71). DSC-rCBF war dem ASL-rCBF mit einer AUC von 0,59 gegenüber 0,58 leicht überlegen. Die Kombination von DSC-rCBV und ASL-rCBF (AUC = 0,71) war dem alleinigen DSC-rCBV ebenbürtig. Der beste prädikative Wert konnte durch eine Kombination von DSC-rCBV, DSC-rCBF, leakage und ASL-rCBF (AUC = 0,74) erzielt werden. DSC- und ASL-rCBF wiesen eine moderate Sensitivität und Spezifität für die Vorhersage der rezidivfreien Intervalle auf. Im Gegensatz zu DSC-rCBV (p = 0,002) unterschieden sich die Werte für die rezidivfreien Überlebenszeit in den Kaplan-Meier-Kurven jedoch nicht signifikant.

Schlussfolgerung

Es konnte weder eine Korrelation noch eine Austauschbarkeit zwischen den DSC-rCBF- und den ASL-rCBF-Werten festgestellt werden. Der prädiktive Wert von ASL-rCBF war zwar mit DSC-rCBF vergleichbar, jedoch nicht signifikant hinsichtlich der Vorhersage der rezidivfreien Überlebenszeit. Die rCBV-Werte wiesen die beste Sensitivität und Spezifität bei der Vorhersage eines Rezidivs sowie der rezidivfreien Überlebenszeit auf. Die Kombination von DSC- und ASL-Perfusionswerten wies vielversprechende Ergebnisse auf, was die

Steigerung des prognostischen Werts beider einzelnstehenden Techniken betrifft.

8. List of publications

8.1. Own published study

Results of this study were already published in the following publication:

M. K. Rau, C. Braun, M. Skardelly, J. Schittenhelm, F. Paulsen, B. Bender, U. Ernemann, S. Bisdas (2014) **Prognostic value of blood flow estimated by arterial spin labeling and dynamic susceptibility contrast-enhanced MR imaging in high-grade gliomas.** *J Neurooncol. 120(3):557-66*

8.2. Declaration of own contribution

The submitted thesis was written by the author (cand. med. Mandy Kim Rau) under the supervision of Prof. Dr. med. Sotirios Bisdas, senior consultant in the the Department of Diagnostic and Interventional Neuroradiology of the University Hospital Tübingen. The MRI exams were carried by the MRI technologists in the Department of Diagnostic and Interventional Neuroradiology of the University Hospital Tübingen. The post-processing of the perfusion-weighted data and the ROI analysis were performed by the author. Tumour volume and enhancing portions of tumour for ROI anaylsis were also assessed and validated from Prof. Dr. med. Sotirios Bisdas. Medical records assessment for time to tumour progression or death, therapy schemes and histological results were assessed by the author under supervision of Prof. Dr. med. Sotirios Bisdas and Dr. med. Christian Braun from the Department of Neurology, who assisted the author in retrieving any clinical information. The publication in Journal of Neurooncology was written by the author under the supervision of Prof. Dr. med. Sotirios Bisdas.

This declaration was signed by all co-authors.

9. Acknowledgement

I’d like to thank my friend Konstanze Alschner not only for her painstaking proofreading, but also for motivating me in times full of doubts.

Moreover I thank Prof. Dr. med. Dipl. Phys. Thomas Nägele and Prof. Dr. rer. nat. Uwe Klose for their support in finalising this work.

Last but not least I thank my family and partner supporting and believing in me through my whole study and work at this doctoral thesis.